Author Manuscript

Author Manuscript

Author Manuscript

Author Manuscript

HHS Public Access

Author manuscript

J Theor Biol. Author manuscript; available in PMC 2016 June 06.

Published in final edited form as:

J Theor Biol. 2013 March 21; 321: 83–99. doi:10.1016/j.jtbi.2012.12.002.

Modeling the interactions of bacteria and Toll-like receptor-mediated inflammation in necrotizing enterocolitis

Julia Arciero[a,*], **G. Bard Ermentrout**[b,e], **Richard Siggers**[c], **Amin Afrazi**[c], **David Hackam**[c], **Yoram Vodovotz**[d,e], and **Jonathan Rubin**[b,e]

[a]Department of Mathematics, IUPUI, Indianapolis, IN 46202, USA

[b]Department of Mathematics, University of Pittsburgh, Pittsburgh, PA 15260, USA

[c]Division of Pediatric Surgery and Department of Surgery, University of Pittsburgh, Pittsburgh, PA 15224, USA

[d]Department of Surgery, University of Pittsburgh, Pittsburgh, PA 15213, USA

[e]Center for Inflammation and Regenerative Modeling, McGowan Institute for Regenerative Medicine, University of Pittsburgh, Pittsburgh, PA 15219, USA

Abstract

Necrotizing enterocolitis (NEC) is a severe disease of the gastrointestinal tract in premature infants, characterized by a disrupted intestinal epithelium and an exaggerated pro-inflammatory response. Since the activation of Toll-like receptor-4 (TLR4) blocks cell migration and proliferation and contributes to an uncontrolled inflammatory response within the intestine, this receptor has been identified as a key contributor to the development of NEC. Toll-like receptor-9 (TLR9) has been shown to sense bacterial genome components (CpG DNA) and to play an anti-inflammatory role in NEC. We present *in vitro* results demonstrating direct inhibition of TLR4 activation by CpG DNA, and we develop a mathematical model of bacteria–immune interactions within the intestine to investigate how such inhibition of TLR4 signaling might alter inflammation, associated bacterial invasion of tissue, and resulting outcomes. The model predicts that TLR9 can inhibit both the beneficial and detrimental effects of TLR4, and thus a proper balance of action by these two receptors is needed to promote intestinal health. The model results are also used to explore three interventions that could potentially prevent the development of NEC: reducing bacteria in the mucus layer, administering probiotic treatment, and blocking TLR4 activation. While the model shows that these interventions would be successful in most cases, the model is also used to identify situations in which the proposed treatments might be harmful.

Keywords

Mathematical model; TLR4; TLR9; Inflammatory response; Intestine

*Corresponding author. Tel.: +1 734 306 8766. ; Email: jarciero@math.iupui.edu (J. Arciero)

Author Manuscript Author Manuscript Author Manuscript Author Manuscript

1. Introduction

Necrotizing enterocolitis (NEC) is a devastating gastrointestinal tract disease that is among the leading causes of neonatal mortality (Guner et al., 2009). The disease primarily affects premature infants, which in part reflects the immature intestinal barrier function and immune/inflammatory responses. In healthy infants, the intestinal epithelial barrier, which separates the contents of the intestinal lumen from the blood and tissue, is intact. In infants with NEC, a compromised epithelial barrier and immature immune response can lead to exaggerated inflammation and bacterial translocation from the intestinal lumen into the circulation, potentially resulting in systemic sepsis and subsequent multi-organ failure (Hunter et al., 2008).

The gut of the newborn is sterile at birth (Gregory et al., 2011). Immediately following birth, the intestinal lumen is colonized with a dense and rapidly diversifying population of bacteria, known as the normal flora, that is essential for the maturation of the immune system and for the developmental regulation of the intestinal physiology (Collado et al., 2012). The first components of the normal flora to appear are facultative anaerobes, such as enterobacteria, coliforms, lactobacilli, and streptococci; these are typically followed by anaerobes, including bifidobacteria, bacteroides, clostridia, and eubacteria. Common bifidobacteria include *B. infantis, B. longum*, and *B. breve*. The mode of delivery (i.e., vaginal or cesarian) as well as nutrition type (i.e., breast fed vs. formula fed) are key factors that cause differential colonization and composition of the neonatal gut (Turroni et al., 2012). Once the normal flora is established in the early years of life, it is thought that this composition of flora is not changed throughout the rest of life (Collado et al., 2012). In general, the normal flora (also known as commensal bacteria) are beneficial for the host and promote health by enhancing digestion efficiency, limiting pathogenic bacterial colonization, and triggering the development and maturation of the immune system. Host defense mechanisms prevent uncontrolled inflammatory responses to commensal bacteria by limiting direct contact between bacteria and the epithelium. Such mechanisms provide immune tolerance to commensal bacteria but trigger an immune response to foreign bacterial populations (Ohland and MacNaughton, 2010). However, since the composition of commensal bacteria populations can vary greatly between helpful and harmful bacteria at various times or within different individuals (Hooper and Macpherson, 2010), the host is challenged with determining the appropriate response to these microorganisms (Duerkop et al., 2009). The mucus layer, intestinal macrophages, and blood macrophages are three important defense mechanisms that help to maintain homeostasis in the gut. However, the inflammatory response by which macrophages eliminate bacteria also can cause collateral tissue damage and must be moderated by anti-inflammatory mechanisms to avoid negative outcomes. An ideal balance of these defense mechanisms should protect the host from invading pathogens across a broad range of conditions, whereas an imbalance that emerges in particular situations, such as in immature states, would result in disease, such as NEC.

Despite the advances that several studies have made to clarify the pathogenesis of NEC, there is still uncertainty regarding how specific gastrointestinal components contribute to the emergence of this multifactorial disease. Although numerous factors must be considered to gain a comprehensive understanding of NEC, studies showing that TLR4 is increased in the

Author Manuscript Author Manuscript Author Manuscript Author Manuscript

bowel of humans with NEC and that TLR4 signaling in the intestinal epithelium is required for NEC (Sodhi et al., 2012) have motivated the use of computational modeling in this paper to explore how enterocyte Toll-like receptors (TLRs), which are activated by membrane components or DNA of bacteria, affect the pathogenesis of NEC. TLR4 molecules sense bacteria and release antimicrobial agents that protect against bacterial translocation (Kubinak and Round, 2012), but they also promote potentially damaging inflammation. Hackam and colleagues have shown that TLR9 molecules suppress TLR4 activation within the newborn small intestinal mucosa, potentially reducing inflammatory damage but also compromising their antibacterial effects (Gribar et al., 2009; Afrazi et al., 2011; Sodhi et al., 2011). Computational modeling offers a means to explore how these competing effects interact, which long-term outcomes are expected in different parameter regimes, and how attempts at therapeutic intervention can influence system dynamics. In the remainder of the introduction, we provide some additional background information on biological components that are relevant to our model. We present the computational model in Section 2. In Section 3, we give results on stable steady state solutions of the model, including how these states depend on key model parameters. We start with a core model lacking TLR4 or TLR9 and subsequently introduce first TLR4 and then TLR9 to the model to illustrate how each of these elements contribute to the system's long-term behavior. The paper concludes with a discussion in Section 4.

1.1. Intestinal mucus layer

A layer of mucus lines the apical side of the epithelium in order to prevent direct contact of luminal bacteria with epithelial cells. This is the first key barrier that intestinal bacteria encounter. The composition of the mucus inhibits effective or rapid movement of bacteria. However, in areas of inflammation, the mucus layer tends to be thinner, often allowing pathogenic bacteria to penetrate the mucus and reach the epithelium (Corazziari, 2009).

Several antimicrobial proteins, such as defensins and cathelicidins, are released into the mucus layer and eliminate bacteria (Duerkop et al., 2009). These proteins are expressed constitutively but are also induced in the presence of bacteria. For example, dendritic (immune) cells residing in the intestinal tissue can extend protrusions through the epithelial layer and sample the bacterial contents of the lumen. If bacteria are sensed, these dendritic cells trigger the release of antimicrobial proteins or IgAs. Antimicrobial proteins promote bacterial killing by compromising the integrity of bacterial cell walls (Ohland and MacNaughton, 2010; Duerkop et al., 2009). Bacteria-specific IgAs are secreted into the intestinal lumen, where they trap pathogens by surrounding them with a hydrophilic shell that is repelled from the epithelium (Ohland and MacNaughton, 2010; Duerkop et al., 2009; Leser and Molbak, 2009). Antimicrobial proteins also target normal microflora in order to prevent an unnecessary or harmful inflammatory response in the gut (Meyer-Hoffert et al., 2008).

1.2. Intestinal and blood macrophages

In some cases, the mucus layer is insufficient to prevent bacterial penetration of the intestinal epithelium or inhibit an inflammatory response against commensal bacteria. Instead, bacteria (pathogenic or commensal) may enter epithelial cells or pass through

Author Manuscript Author Manuscript Author Manuscript Author Manuscript

spaces between them. Ideally, these bacterial invaders will be eliminated by intestinal macrophages, which are macrophages positioned in the intestinal lamina propria that respond directly to the presence of bacteria in the intestinal tissue. Intestinal macrophages can phagocytose and kill microorganisms but do not release pro-inflammatory cytokines in large quantities, unlike macrophages in other tissues (Smith et al., 2005; Smythies et al., 2005). In this way, bacteria may be eliminated without causing much damage to the gut (Smith et al., 2005). However, it is hypothesized that intestinal macrophages are dysfunctional in very low birth weight infants, contributing to increased bacterial translocation (Sherman, 2010). In particular, in the normal fetus, intestinal macrophages undergo progressive inflammatory down-regulation, but in the case of preterm deliveries, this down-regulation is incomplete, resulting in an increased risk of a severe inflammatory response to bacteria (Maheshwari et al., 2011).

If neither the mucus layer nor intestinal macrophages is effective at preventing bacteria from entering the blood and tissue, an overly robust inflammatory response ensues, including the activation of blood macrophages and the systemic secretion of pro-inflammatory cytokines. An inflammatory response is necessary to destroy harmful bacteria, but inflammation also causes injury to the intestinal barrier and inhibits epithelial cell proliferation and migration. Thus, as a result of a widespread pro-inflammatory response, the rate of bacterial translocation may be increased and the ability to repair the intestinal barrier may be impaired.

1.3. TLR4 and TLR9 signaling

TLR4 is expressed on both the apical and basolateral surfaces of enterocytes (intestinal epithelial cells) and can facilitate bacterial translocation across the epithelium (Neal et al., 2006). TLR4 is the main receptor for lipopolysaccharide (LPS), which is a component of the outer membrane of Gram-negative bacteria. Gram-negative bacteria are the primary type of bacteria that have been identified as being central to the pathogenesis of NEC (Hunter et al., 2008). If the mucus layer and intestinal macrophage defense mechanisms are not successful at preventing bacterial translocation, the activation of TLR4 by LPS can result in a widespread pro-inflammatory response. In particular, following TLR4 activation, the nuclear factor κ-light-chain-enhancer of activated B cells (*NF*-κB) is translocated to the nucleus. This signaling cascade can trigger the secretion of antimicrobial factors and IgAs (Duerkop et al., 2009; Vaishnava et al., 2008) as well as the production and release of various pro-inflammatory cytokines (Xavier and Podolsky, 2000). If an overwhelming inflammatory response occurs, increased damage and bacterial translocation typically result and contribute to the development and severity of NEC.

TLR4 expression is significantly elevated in the bowels of humans with NEC (Chan et al., 2009) and in experimentally induced NEC, relative to control conditions (Leaphart et al., 2007). If TLR4 is blocked, bacterial translocation is reduced significantly (Neal et al., 2006). In fact, Leaphart et al. (2007) observed that in mice whose TLR4 signaling was blocked (TLR4-mutant mice, in which the gene coding for TLR4 contains a point mutation that nullifies downstream intracellular signaling), there was no response to LPS. Experiments have provided a measure of NEC severity in the presence or absence of TLR4 (Gribar et al.,

Author Manuscript Author Manuscript Author Manuscript Author Manuscript

2009). In wild type mice, NEC severity was between 2 and 3 (severe), but in TLR4-mutant mice, NEC severity was nearly 0 (normal) (Leaphart et al., 2007). Interestingly, levels of TLR4 expression in the gut increase prior to birth and do not decrease to a normal level until the day of birth (Gribar et al., 2009), which could partly explain the primary development of NEC in preterm infants. Similarly, Lotz et al. (2006) noted rapid TLR4 signaling after LPS stimulation in fetal intestinal epithelial cells (IECs) that was completely absent from adult IECs. Claud et al. (2004) observed significantly higher pro-inflammatory cytokine secretion in response to bacterial infection in immature IECs compared with mature IECs, likely due to the increased TLR4 activity in immature enterocytes.

Repair of the injured epithelial layer requires the efficient migration of epithelial cells into the site of injury. TLR4 activation increases the adhesion of enterocytes to the underlying matrix, which in turn restricts normal cell migration. For example, in a scrape wound assay of intestinal epithelial cells, migration was normal under control conditions but significantly impaired in the presence of LPS (Leaphart et al., 2007). TLR4 activation inhibits enterocyte proliferation (Sodhi et al., 2010), which is a process that is also needed for normal injury repair. These observations suggest that TLR4 activation contributes to intestinal injury and also inhibits healing (Leaphart et al., 2007; Qureshi et al., 2005; Afrazi et al., 2011).

Although several harmful effects of TLR4 have been identified related to cell migration and the inflammatory response, the majority of infants express TLR4 but do not develop NEC. When expressed at a normal level, TLR4 signaling plays an important role in establishing optimal proliferation and protection against apoptosis in the colon (Afrazi et al., 2011; Sodhi et al., 2011). It has been hypothesized that the connection between TLR4 and the development of intestinal inflammation is influenced by multiple factors, including the type of effector cells, developmental factors, and region of the intestine (Afrazi et al., 2011). Moreover, TLR4 signaling has been shown to protect against pathogenic infections as well as to induce tolerant responses to commensal bacteria (Kubinak and Round, 2012). Thus, the means by which TLR4 responsiveness is maintained at an appropriate level to maintain homeostasis and host protection is an important topic for both experimental and computational investigation.

TLR9 is a Toll-like receptor that recognizes demethylated DNA, which is DNA that contains several CpG motifs (regions of DNA where a cytosine nucleotide occurs next to a guanine nucleotide, separated by only one phosphate). These motifs are characteristic of the bacterial genome and hence serve to alert the host to the presence of bacterial infection. Studies have shown that TLR9 activation with CpG DNA can limit TLR4 signaling in enterocytes and reduce intestinal inflammation in NEC (Gribar et al., 2009; Sodhi et al., 2011), unlike the activation of inflammation by TLR9 in other contexts. Interestingly, TLR9 and TLR4 are reciprocally expressed in the developing intestine (Gribar et al., 2009). That is, when TLR4 levels are high (pre-birth), TLR9 levels are very low, whereas at birth TLR9 levels are elevated and TLR4 levels are low.

Gribar et al. (2009) explored the potentially beneficial effects of altering the expression of TLR4 and TLR9 in the infant intestine. CpG DNA attenuated TLR4 signaling in enterocytes (but not in inflammatory cells), and the amount of bacterial translocation to mesenteric

Author Manuscript Author Manuscript Author Manuscript Author Manuscript

lymph nodes decreased significantly when CpG DNA was added to intestinal epithelial cells treated with LPS. Moreover, activation of TLR9 by CpG DNA reduced the severity of experimental NEC (Gribar et al., 2009). These observations suggest that promoting the activation of TLR9 may be a strategy for treating infants with NEC. It is hypothesized that probiotics (nonpathogenic bacteria species that are beneficial to the host and are the same species that comprise the normal flora of the gut and breast milk) may be a successful treatment for NEC in part because probiotic bacterial DNA can activate TLR9, which in turn inhibits the activation of TLR4. Another potential beneficial mechanism of probiotics involves their interference with the activation of NF-κB in gut epithelial cells. In particular, commensal bacteria (and probiotics) have been shown to inhibit the translocation of *NF*-κB into the nucleus, thereby blocking the release of pro-inflammatory cytokines (Xavier and Podolsky, 2000; Neish et al., 2000).

1.4. Computational model

The transfer of nutrients, growth factors, and immunoglobulins from mother to child, which would normally protect the infant from bacteria that colonize the intestinal tract, is interrupted in infants born prematurely (Edde et al., 2001). As a result, these premature infants often experience sustained inflammation and bacterial translocation, which can lead to severe diseases. The majority of premature infants never progress to NEC, although up to 15% of all low birth weight, premature infants have been shown to develop NEC (Lin et al., 2008b). Mathematical models (Arciero et al., 2010; Reynolds et al., 2006; Kim et al., 2012) combined with experimental observations (Gribar et al., 2009; Hackam et al., 2005) can be used to investigate potential physiological mechanisms and developmental factors that contribute to NEC and to identify possible treatment strategies for the disease. Importantly, these models are designed to include factors that may contribute to the pathophysiology of NEC, but they predict a wide range of health and disease states that are consistent with the clinical observation that NEC often does not develop even among its most susceptible population in the majority of cases. A previous theoretical model was focused on predicting and understanding the factors that contribute to NEC (Kim et al., 2012); the focus of the current study is to evaluate components of the inflammatory response that may impact the development of NEC. In particular, the model presented in this study is used to predict conditions under which TLR4 and TLR9 activation affect health or disease outcomes for a premature infant. The model represents the interactions between a bacterial population and certain major elements of the immune response in the mucus layer and intestinal tissue. We consider several levels of model complexity, sequentially adding components to identify how they contribute to long-term outcomes.

2. Methods

2.1. Model development

A system of ordinary differential equations is used to track the number of bacteria in the mucus layer of the intestine and in a combined blood/tissue compartment, the rate of bacterial translocation from intestine to blood/tissue, and the effects of macrophage activation and inflammation, which are provoked by bacteria. The present model is based on our previously published work (Arciero et al., 2010). Our prior mathematical model was

Author Manuscript Author Manuscript Author Manuscript Author Manuscript

altered to include immune mechanisms in the mucus layer that help to limit direct contact between bacteria and the epithelium (Hooper and Macpherson, 2010; Lan et al., 2005) as well as mechanisms for the activation and interaction of enterocyte TLR4 and TLR9. The focus of our study is the investigation of TLR effects on the combined mucus/blood/tissue system in the context of NEC. In a departure from our previous model (Arciero et al., 2010), an intestinal lumen compartment is not explicitly included in this model; instead, bacteria are assumed to enter the mucus layer from the lumen at a fixed rate. Also, the population of inflammatory cells tracked in Arciero et al. (2010) is replaced by a pro-inflammatory cytokine population in this study. This simplification of considering the immune response as a lumped response is sufficient for the purposes of this model but could be altered in the future to include more detailed interactions between immune cells and cytokines. A schematic illustration of the model compartments and quantities tracked in the model is given in Fig. 1A, and model dynamics are depicted in Fig. 1B.

2.1.1. Mucus layer compartment—The dynamics of the number of bacteria in the mucus layer (B_M) is described by Eq. (1)

$$\frac{dB_M}{dt}=B_{M,\text{source}}-\frac{k_{AD}B_M}{k_3+B_M}-\frac{k_{AT}R_EB_M}{\alpha_{EM}+R_E}-\varepsilon B_M. \quad (1)$$

According to this equation, bacteria enter the mucus layer from the intestinal lumen at a constant rate $B_{M,source}$ (Duerkop et al., 2009). Increasing this parameter value in Eq. (1) signifies an increase in bacteria in the system and can be used to simulate differing degrees of infection. Using a constant positive value for $B_{M,source}$ is reasonable since bacteria are always present in the mucus. A larger value of $B_{M,source}$ could be used to represent ischemic injury, which is typical at least in some animal models of NEC and causes the mucus layer to be permissive to bacteria.

Dendritic cells sample the contents of the mucus layer and are effective at killing phagocytosed bacteria (Smith et al., 2005; Hooper and Macpherson, 2010) at a rate that we treat as saturating, based on the finite size of the dendritic cell population. In the second term of Eq. (1), we combine this effect with the destruction of bacteria in the mucus layer by antimicrobial proteins; for example, after an *E. coli* infection was induced in rat intestine, bacterial translocation into the blood and liver was significantly lower in rats given lactoferrin (an antimicrobial protein present in mother's milk) than in control-treated rats (Edde et al., 2001). We note that the amount of mRNA coding for antimicrobial proteins increases with development stage, with the least amount in the fetus and the highest amount in the adult (Hecht, 1999). This observation clearly contributes to the susceptibility of premature infants to NEC. The parameter value used for k_{AD} in this model is smaller than the value that would be used in a corresponding adult model of intestinal interactions.

TLR4 molecules respond directly to LPS. We do not explicitly track LPS in the model, but the third term in Eq. (1) represents the effects of TLR4 activation by LPS on mucus layer bacteria. Specifically, if activated TLR4 molecules (represented by variable R_E in the model) sense bacteria (LPS) in the mucus layer, the TLR4 molecules trigger the release of

Author Manuscript Author Manuscript Author Manuscript Author Manuscript

antimicrobial substances into the mucus to destroy bacteria. A saturated form for this term is chosen to reflect the limited ability of TLR4 to trigger this antimicrobial release.

Some bacteria are able to penetrate the mucus and enter the blood and tissue by crossing the epithelial layer (Deitch, 1994), as has been observed in both animal (Wenzl et al., 2001) and human studies (Papoff et al., 2012; Deitch, 1989). The rate of translocation is given by variable ε, which appears in the fourth term in Eq. (1). The rate of bacterial translocation across the epithelial layer tends to be higher in premature infants due to incomplete development of the epithelium as well as damage to the layer caused by an exaggerated inflammatory response, as we discuss next.

2.1.2. Epithelial cell layer—The rate of bacterial translocation, ε, evolves according to Eq. (2)

$$\frac{d\varepsilon}{dt}=\frac{\varepsilon_0-\varepsilon}{\tau}+fP(\varepsilon_{\max}-\varepsilon). \quad (2)$$

A nonzero rate of translocation (ε_0) is specified for the intestinal epithelium under baseline conditions (first term), as in Arciero et al. (2010). If the intestinal epithelium is injured, the bacteria are able to breach the epithelial barrier more easily (Samel et al., 2002). Bacterial translocation across the epithelium initiates a full-blown immune response, which can cause additional damage to the epithelial layer and promote a positive feedback cycle between inflammation and damage. The risk factors for bacterial translocation are also risk factors for NEC, especially an impaired epithelial barrier. To assess how bacterial translocation contributes to the pathogenesis of NEC, the model includes a simplified representation of the effects of inflammation on bacterial translocation. Specifically, the rate of translocation in the model is increased in the presence of blood/tissue pro-inflammatory cytokines, *P*, with a gain *f*, since cytokines initiate and sustain an inflammatory response that damages the intestinal epithelium (Edelson et al., 1999; Bianchi and Manfredi, 2009). Although antiinflammatory cytokines are not explicitly included in this model, parameter *f* is also assumed to take into account the inhibitory action of anti-inflammatory cytokines.

Activated TLR4 molecules (R_E) and TLR9 molecules (I_E) on the epithelium are represented in the model using Eqs. (3) and (4)

$$\frac{dR_E}{dt}=\frac{a_1B_MT_I}{(\gamma_1+B_M)(1+\alpha_{RE}I_E)}+\frac{k_1P}{1+\alpha_{RE}I_E}-\mu_{RE}R_E, \quad (3)$$

$$\frac{dI_E}{dt}=\frac{k_{IE}R_E}{\gamma_{IE}+R_E}+\alpha_{11}B_M-\mu_{IE}I_E. \quad (4)$$

The ligands recognized by TLRs are not specific to pathogenic bacteria, and thus commensal bacteria may also activate TLRs (Rakoff-Nahoum et al., 2004). The first and second terms of

Author Manuscript Author Manuscript Author Manuscript Author Manuscript

Eq. (3) represent TLR4 activation in the presence of bacteria (LPS) and pro-inflammatory cytokines, respectively. Specifically, term 1 of Eq. (3) defines the activation of a constant, inactive TLR4 population, T_I, by B_M. Blood/tissue pro-inflammatory cytokines, P, can trigger signaling processes that may affect TLR4 expression (term 2). Enterocyte TLR9 molecules (denoted by I_E) appear in the denominator of these terms to encode the inhibitory effect of TLR9 on TLR4 activation. An ongoing decay of activated TLR4 molecules is also assumed (third term).

The method by which TLR9 (I_E) is activated has been debated in the literature (Ivory et al., 2008; Hackam et al., 2005), and thus two methods of TLR9 activation are included in the model (Eq. (4)). Specifically, TLR9 molecules may be activated intracellularly once bacteria have been internalized by TLR4 (first term) or extracellularly in the presence of bacteria in the mucus layer (second term). In term 2, α_{11} is small, and so we use a linear term to approximate a saturating term. A natural decay of these receptors is also assumed (term 3).

2.1.3. Blood/tissue compartment—Eq. (5) gives the rate of change of bacteria in the blood/tissue compartment (B)

$$\frac{dB}{dt}=[\varepsilon B_M - T]_+ - k_5 PB. \quad (5)$$

A numerical threshold T, which was introduced in a previous model (Arciero et al., 2010), is used in the first term of Eq. (5) to represent the translocation of bacteria across the epithelium into the blood/tissue as well as the effects of intestinal macrophages, which are not explicitly tracked in the model. The threshold term included here is identical to that used previously (Arciero et al., 2010)

$$[x]_+=\max(0,x); \quad (6)$$

that is, bacteria in the mucus are assumed to be internalized only once the product of B_M and ε exceeds a certain threshold value (given by parameter T) (Hooper and Macpherson, 2010). If the product does not exceed the threshold, the bacteria that exit the mucus layer are assumed to be eliminated in the epithelium by intestinal macrophages and prevented from entering the blood compartment. Although separate populations for pathogenic and commensal bacterial species are not defined in this model as they were in Arciero et al. (2010), the use of a threshold function takes into account that the continuous exposure of the epithelium to commensal bacteria in the mucus layer does not trigger a destructive immune response. Experimental observations by Han et al. (2004) provide support for using a threshold function since bacterial translocation behaved like a step function, remaining negligible over a wide range of bacterial population sizes before becoming significant at large population levels. Intestinal macrophages do not produce pro-inflammatory cytokines (Smythies et al., 2005; Lotz et al., 2006; Smith et al., 2005), and thus an inflammatory response is not evoked by this mechanism and a simple representation of intestinal macrophage effects is reasonable. If the threshold T is exceeded, then bacteria enter the

Author Manuscript Author Manuscript Author Manuscript Author Manuscript

blood and are eliminated by blood macrophages (here assumed to be proportional to pro-inflammatory cytokines, P) at rate k_5 (second term in Eq. (5)).

Note that alternative, smooth functional forms of the threshold term could be chosen to achieve the same effect. For example, using $(\varepsilon B_M - T)/(1 - e^{-\beta(\varepsilon B_M - T)})$ in place of $[\varepsilon B_M - T]_+$ gives the same qualitative results. We used the latter function so that the model can generate solutions in which no bacteria enter the blood/tissue compartment, which makes it easy to classify aseptic outcomes. If the max function (Eq. (6)) were not used, then a very small amount of bacteria would always enter the blood/tissue compartment, and we would lose this unambiguous differentiation between aseptic and septic outcomes.

Blood cytokine levels are typically elevated in infants suffering from NEC, and it is hypothesized that studying the pattern of cytokine expression will yield important insights into the pathophysiology of the disease (Edelson et al., 1999; Harris et al., 1994). The rate of change of pro-inflammatory cytokines in the blood/tissue compartment is given by Eq. (7)

$$\frac{dP}{dt} = \frac{k_{PM} B}{\gamma_{12} + B} + \frac{k_{PE}[R_E - T_{RE}]_+}{1 + \gamma_{PE} I_E} - \mu_4 P. \quad (7)$$

Pro-inflammatory cytokine production is activated by bacteria in the blood (first term in Eq. (7)) (Haller et al., 2000; Lan et al., 2005; Gribar et al., 2009; Ivory et al., 2008). A TLR4 threshold, T_{RE}, is introduced in the second term of Eq. (7), using the max function (Eq. (6)). If the number of TLR4 molecules that are activated exceeds T_{RE}, then a full inflammatory response is triggered, leading to cytokine production (Akira et al., 2001; Lotz et al., 2006; Edelson et al., 1999; Smith et al., 2005). If the level of activated TLR4 molecules is below T_{RE}, then $[R_E - T_{RE}]_+ = 0$, such that TLR4 molecules sense bacteria in the mucus and antimicrobial protein production is triggered, but an overly robust inflammatory response does not ensue. A natural decay of cytokines is also assumed (third term in Eq. (7)).

2.2. Experimental procedure

2.2.1. TLR4 and TLR9 staining in IEC6 and RAW cells—IEC6 enterocytes and RAW macrophages (a mouse leukaemic monocyte macrophage cell line commonly used for *in vitro* work studying macrophage biology) were plated upon glass coverslips. Enterocytes were treated with LPS (50 μg/ml) and CpG (4 μM) either separately or simultaneously, and TLR4 and TLR9 expression were subsequently assessed, at 4, 8, and 16 h. Cells were stained for both TLR4 and TLR9 via immunofluroesence. Briefly, cells were fixed in 4% Paraformaldehyde for 20 min followed by 20 min in 0.1% Triton-X solution. Non-specific binding was blocked with 1% BSA 0.15 M Glycine 5% donkey serum for 1 h. Cells were stained with primary antibodies for TLR4 and TLR9 (Imgenex) at 1:100 for 1 h. Cells were washed 3 × with PBS and treated with fluorescent secondary antibodies for detection. Stained coverslips were imaged on a Zeiss LSM 710 confocal microscope to perform imaging using Zen 2009 software.

2.2.2. PCR analysis—IEC6 enterocytes and RAW macrophages were plated upon glass coverslips. Enterocytes were treated with either LPS (50 μg/ml) and CpG (4 μM) separately

Author Manuscript Author Manuscript Author Manuscript Author Manuscript

or simultaneously at various timepoints between 4 and 16 h. Cells were harvested and subjected to RNA isolation using a RNeasy RNA isolation kit (Qiagen). cDNA transcripts were made via Reverse Transcriptase kits (Qiagen). RT-PCR analysis was performed using an iQ5 CFX96 Real-time system Thermocycler (Bio-Rad). The primers that were utilized are listed in Table 1, where F denotes the forward sequence and R denotes the reverse sequence. Multiple comparison procedures were conducted on the PCR data using one-way ANOVA followed by Dunn's post hoc test.

2.3. Parameter values

The model parameters represent rates and relative magnitudes of different types of interactions of bacteria with TLR4, TLR9, and inflammatory cells. Values for several parameters, including ε_0, ε_{max}, k_5, τ, and f, were taken directly from related earlier works (Arciero et al., 2010; Reynolds et al., 2006). Other parameter values were varied over a wide range to assess different behaviors that can be generated by the model. Since this study aims to explore the range of biologically feasible outcomes of the immune response to lumenal bacteria rather than to fit a specific data sample, an optimization procedure is not used to select a specific set of parameter values. However, our results are biologically relevant because the mechanisms included in the model are all directly based on experimental and clinical observations. Table 2 provides a list of parameter values, units, and descriptions for the model, given by Eqs. (1)–(7).

3. Results

Experimental studies have identified TLR4 as a significant factor contributing to the pathogenesis of NEC (Gribar et al., 2009; Sodhi et al., 2010; Afrazi et al., 2011). Specifically, TLR4 activation leads to increased death of epithelial cells, reduced capacity for intestinal cell migration and proliferation, and increased inflammation. The deleterious effects of TLR4 have been shown to be dampened by the activation of TLR9 (Gribar et al., 2009; Afrazi et al., 2011; Leaphart et al., 2007). In this study, the time course of TLR4 expression was measured in lysates of IEC6 cells in the presence or absence of LPS and CpG DNA. TLR4 is the main receptor for LPS, and TLR9 is the main receptor for CpG DNA. The enterocytes are not from an immature cell line, but, based on this data and additional experimental evidence (Sodhi et al., 2012; Gribar et al., 2009; Liu et al., 2009), we hypothesize that the relationships observed here will also apply to, and perhaps be more pronounced in, immature enterocytes. The asterisk above the 16 h data in Fig. 2 is used to indicate that there is a significant difference between TLR4 expression in the presence of LPS at 16 h and TLR4 expression in the presence of LPS + CpG at 16 h ($p < 0.05$), identifying an inhibitory effect of TLR9. In addition, at 16 h, the TLR4 LPS + CpG expression level is not significantly different from media (control). Overall, the experimental data provide evidence for the increased TLR4 expression in the presence of LPS and the decreased expression of TLR4 due to the inhibitory effects of CpG DNA (TLR9).

With these studies and observations as motivation, we used our computational model to elucidate the specific contributions of TLR4 and TLR9 to the dynamics of quantities

Author Manuscript Author Manuscript Author Manuscript Author Manuscript

relevant to NEC and to the long-term steady states achieved. As outlined in Fig. 3, the model was used to investigate the range of possible outcomes in the following three cases:

1. no TLR4, no TLR9;
2. with TLR4, no TLR9;
3. with TLR4, with TLR9.

In this study, an outcome is defined as healthy if no bacteria are present in the blood ($B = 0 \times 10^6$ cells/g) and if the rate of bacterial translocation is at its baseline value ($\varepsilon = \varepsilon_0$) at steady state. To be consistent with existing literature, we classify disease states as aseptic death or septic death (Reynolds et al., 2006; Arciero et al., 2010). An aseptic death outcome corresponds to no bacteria in the blood ($B = 0 \times 10^6$ cells/g) but an elevated rate of bacterial translocation at steady state ($\varepsilon > \varepsilon_0$), implying sustained inflammation. Increased inflammation, and hence an increased rate of bacterial translocation (above baseline), may occur due to increased TLR4 activation; despite this, bacteria will not successfully enter the blood/tissue compartment if the threshold (T) is not exceeded, often due to the elimination of bacteria that breach the epithelial barrier by intestinal macrophages. Septic death is defined as a steady state with bacteria present in the blood ($B > 0 \times 10^6$ cells/g). Although the exact relation between model predictions and clinical diagnoses is not established here, model predictions of aseptic and septic death may roughly represent beginning stages of NEC and full-blown cases of NEC, respectively. As indicated in Fig. 3, health or disease can emerge in the model due to the effects of TLR4, and the additional inclusion of TLR9 can push the system toward health or disease depending on the balance of model components. The conditions that determine the steady state behavior of the model will be explored across these three cases.

3.1. Case 1: absence of both TLR4 and TLR9

In the absence of TLR4 (R_E) and TLR9 (I_E), the model includes killing of mucus layer bacteria by dendritic cells, bacterial translocation from the mucus layer to the blood/tissue if the combined mucus layer bacterial population and epithelial permeability becomes sufficiently large, and a pro-inflammatory response to the presence of bacteria in the blood/tissue, which eliminates bacteria but also increases epithelial permeability. To assess the contributions of TLR4 and TLR9 to system dynamics, it is useful to first see how this reduced system behaves. With R_E and I_E pinned at 0, the model simplifies to a system of four differential equations, corresponding to the NEC model in an earlier work (Arciero et al., 2010). The system can be further reduced to two ODEs, for B_M and ε, if we make a quasi-steady state approximation and set P and B to be functions of εB_M that satisfy $dB/dt = dP/dt = 0$. This reduction does not alter the number and values of the equilibria, but it could alter their stability (we note that it does not in fact alter the stability here).

The resulting nullclines for B_M and ε are shown in Fig. 4. To generate the ε nullcline, we consider two components. For one component, we have $\varepsilon = \varepsilon_0$, $P = 0$, and $B = 0$. These conditions indeed give $dB/dt = dP/dt = d\varepsilon/dt = 0$ as long as $\varepsilon_0 B_M < T$, so this component is defined for $B_M \in [0, T/\varepsilon_0)$. The other component corresponds to $\varepsilon > \varepsilon_0$ with $P, B > 0$, which requires $\varepsilon B_M > T$. The number and location of intersections of the ε and B_M nullclines (i.e.,

Author Manuscript Author Manuscript Author Manuscript Author Manuscript

critical points) depend on the model parameter values. Here, the effects of $B_{M,source}$, representing the intensity of the bacterial invasion, and k_{AD}, encoding the effectiveness of the dendritic cell response, are examined. In each panel of Fig. 4, the dashed black curve corresponds to $\varepsilon B_M = T$. Three possible dynamics for Case 1 are depicted in Fig. 4: a single healthy steady state, bistable steady states, or a single disease steady state. Each of these cases arises over a range of $B_{M,source}$ and k_{AD} values.

In the first column (Fig. 4A and D), the B_M nullcline (blue) intersects the ε nullcline (red) at one point along the line $\varepsilon = \varepsilon_0$. This steady state is healthy since the rate of bacterial translocation at steady state is at its baseline value ($\varepsilon = \varepsilon_0$) and the intersection point of the nullclines is located to the left of (below) the dashed black curve, indicating that $\varepsilon B_M < T$ at steady state, as needed for consistency. This configuration and an associated stable health state are predicted to arise for 0×10^6 cells/g/h $\leq B_{M,source} \leq 1.65 \times 10^6$ cells/g/h (when $k_{AD} = 1 \times 10^6$ cells/g/h). The B_M nullcline plotted in Fig. 4A and D depicts the largest value of $B_{M,source}$ (to within 0.01×10^6 cells/g/h) within that range. The shaded region in panel A corresponds to shifted positions of the B_M nullcline that would still yield health.

The second column of Fig. 4 (Fig. 4B and E) illustrates a configuration, which occurs for values of $B_{M,source}$ in the range 1.66×10^6 cells/g/h $\leq B_{M,source} \leq 1.74 \times 10^6$ cells/g/h (with $k_{AD} = 1 \times 10^6$ cells/g/h), that yields a prediction of bistability, as indicated by the three intersection points of the nullclines. Two B_M nullclines (blue), one for $B_{M,source} = 1.66 \times 10^6$ cells/g/h and the other for $B_{M,source} = 1.74 \times 10^6$ cells/g/h, are shown in Fig. 4B to outline the region where B_M nullclines that give bistability may lie. In this region (shaded), the prediction of a health or septic death outcome depends on the initial value of B_M. For example, for values of $B_{M,source}$ in this range, if $B_M(0) = 0 \times 10^6$ cells/g, health is predicted, but if $B_M(0) = 20 \times 10^6$ cells/g, a disease steady state is predicted. Note that intersection points on $\varepsilon = \varepsilon_0$ lie to the left of/below the curve $\varepsilon B_M = T$, while intersections with $\varepsilon > \varepsilon_0$ lie to the right of/above this curve, such that all are self-consistent.

Finally, in the third column (Fig. 4C and F), the single intersection point corresponds to a septic death prediction when $B_{M,source} \geq 1.75 \times 10^6$ cells/g/h ($k_{AD} = 1 \times 10^6$ cells/g/h). In this shaded region, the B_M nullcline will always intersect the upper branch of the ε nullcline once, corresponding to an elevated rate of bacterial translocation ($\varepsilon > \varepsilon_0$) and presence of bacteria in the blood ($\varepsilon B_M > T$). The second row of Fig. 4 provides a zoomed version of the graphs in the top row to depict how the system behavior for the three ranges of $B_{M,source}$ results from the shape and location of the nullclines with respect to the threshold curve.

In Case 1, septic death is predicted when the threshold T is exceeded, implying either B_M or ε has increased sufficiently for their product to exceed and remain above threshold at steady state. The parameter values chosen for $B_{M,source}$, k_{AD}, or k_{PM} affect whether or not this threshold is crossed. If the rate of entrance of bacteria into the mucus layer, $B_{M,source}$, is increased (as would occur with the introduction of an infection), the B_M nullcline shifts to the right and steady states may be created through a saddle-node bifurcation to yield bistability (Fig. 4B) or may merge through a subsequent saddle-node bifurcation to ensure septic death (Fig. 4C).

Author Manuscript Author Manuscript Author Manuscript Author Manuscript

A decrease in k_{AD} will also cause the B_M nullcline to shift to the right. A low value of k_{AD} corresponds to a weak response by dendritic cells, causing bacterial levels in the mucus layer to remain high. The effects of varying $B_{M,source}$ or k_{AD} are summarized with three sample nullclines in the $\varepsilon - B_M$ phase plane in Fig. 5A. Health and disease predictions are summarized in k_{AD}–$B_{M,source}$ parameter space in Fig. 5B. The two curves in Fig. 5B separate health and septic death regions for initial conditions of $B_M(0) = 0 \times 10^6$ cells/g (blue) and $B_M(0) = 20 \times 10^6$ cells/g (magenta). Points to the left of each curve are combinations of parameter values for which the corresponding initial condition yields a healthy steady state outcome, whereas for points to the right of each curve, this initial condition gives a septic death outcome. The points in between the two curves correspond to the region of bistability, since health is predicted for $B_M(0) = 0 \times 10^6$ cells/g but septic death is predicted for $B_M(0) = 20 \times 10^6$ cells/g in this region.

Increasing k_{PM} corresponds to an immune system that is increasingly sensitive to bacteria in the blood. As k_{PM} is increased, the ε nullcline shifts upward and changes shape, causing the number of steady states to increase from one to three. Two ε nullclines corresponding to increasing values of kPM are shown in the phaseplane in Fig. 5C. While a strong immune response is often thought to be beneficial, it also causes increased damage to the epithelial layer. Thus, increased sensitivity of the immune response can transform a system from a potentially healthy state to a disease state. Fig. 5D gives a summary of health, aseptic death, and septic death predictions in the $k_{PM} - B_{M,source}$ parameter space when $B_M(0) = 20 \times 10^6$ cells/g. If $B_M(0) = 0 \times 10^6$ cells/g, increasing k_{PM} does not change the steady state prediction of health for the parameter ranges shown in the figure, and thus this case is not depicted in Fig. 5D.

3.2. Case 2: presence of TLR4 and absence of TLR9

Since TLR4 has been shown to be a key contributor to NEC (Gribar et al., 2009; Hackam et al., 2005; Sodhi et al., 2010), the previous NEC model in Arciero et al. (2010) is extended to include several mechanisms by which TLR4 (R_E, see Eq. (3)) acts. To isolate the effects of TLR4 in the system that are independent of TLR9, we set $I_E = 0$, and the model reduces to a system of five differential equations (Eqs. (1)–(5)).

As in Case 1, all of the model equations in Case 2 can be expressed at steady state in terms of B_M and ε. The B_M nullcline and ε nullcline can be used to assess changes in the possible steady states of the model, as illustrated in Fig. 6 (color-coding as in Fig. 4). The nullclines shown in Fig. 6A correspond to the case when neither threshold is crossed (i.e., $\varepsilon B_M < T$ and $R_E < T_{RE}$), and a healthy steady state is predicted. Note that although the T_{RE} threshold cannot be explicitly depicted in the $\varepsilon - B_M$ phase plane, we use direct simulations of the model to determine whether or not T_{RE} has been crossed.

In the center panel (Fig. 6B), the slope of the ε nullcline is positive, and the nullclines intersect at a point at which $\varepsilon > \varepsilon_0$. This indicates that there is sustained inflammation in the system, which occurs because $R_E > T_{RE}$. Since the εB_M product (at steady state) is to the left of the black dashed curve, this panel depicts an aseptic death prediction: no bacteria remain in the blood at steady state but $\varepsilon > \varepsilon_0$. The curves depicted in panels A and B were generated under the assumption $\varepsilon B_M < T$, and a portion of the ε nullcline is colored grey in each to

Author Manuscript Author Manuscript Author Manuscript Author Manuscript

illustrate a region that is inconsistent with this assumption. In Fig. 6C, both thresholds are exceeded and a septic death outcome is predicted regardless of $B_M(0)$.

The results in Fig. 6 were generated using a single k_{AD} value ($k_{AD} = 1 \times 10^6$ cells/g/h); in Fig. 7, parameters k_{AD}, $B_{M,source}$, and a_1 are varied to determine their effects on model predictions in the presence of TLR4. Parameter k_{AD} is the rate at which dendritic cells and antimicrobial proteins destroy bacteria in the mucus layer. This parameter is varied since the success of this immune response may vary with developmental stage. Parameter $B_{M,source}$ is varied to reflect differing degrees of infection. In Fig. 7A, increasing $B_{M,source}$ (or decreasing k_{AD}) causes a rightward shift in the B_M nullcline and a simultaneous upward shift of the ε nullcline. Moderate increases in $B_{M,source}$ cause an increased inflammatory response such that R_E exceeds the T_{RE} threshold, leading to an aseptic death prediction. Significant increases in $B_{M,source}$ cause εB_M to increase above T due to both increased inflammation and bacteria entering the mucus layer; once T is exceeded, septic death is predicted by the model. A summary of health, aseptic, and septic death predictions is shown in Fig. 7B in $k_{AD} - B_{M,source}$ parameter space. The results from Case 1 are also provided (blue) to illustrate that the health region predicted in the absence of TLR4 shrinks substantially and that the previously healthy parameter sets yield aseptic outcomes when the roles of TLR4 are considered (Case 2). As in Fig. 5B, regions to the left and right of the curves are labeled as health, aseptic, or septic.

The results in Fig. 7A–B are given for a fixed activation rate of TLR4 (a_1 = 0.1/h). However, these outcomes are sensitive to variations in the rate of bacterial activation of TLR4 (a_1). Fig. 7C shows the upward shift in the ε nullcline as a_1 is increased ($B_{M,source} = 1.6 \times 10^6$ cells/g/h). The ε nullcline saturates near ε_{max} = 0.21/h as a_1 is increased, demonstrating that uncontrolled activation of TLR4 leads to overwhelming inflammation, which is a characteristic of NEC. The $k_{AD} - B_{M,source}$ parameter space in Fig. 7D includes the effect of increasing a_1 (a_1 = 0.1/h (green) and 0.5/h (magenta)). The blue curve included in the figure shows the division between health and septic death when TLR4 is absent (Case 1). The point labeled A represents combinations of parameter values that would yield a healthy outcome in Case 1 but an aseptic outcome for Case 2. Point B corresponds to a case that was septic for Case 1 and aseptic in Case 2. Interestingly, increasing a_1 significantly impacts predictions of health by converting a large previously healthy parameter region into an aseptic region due to its effect of increasing inflammation in the system. However, increasing a_1 only weakly affects the boundary between aseptic and septic states, converting some borderline aseptic parameter sets to septic outcomes by yielding increased epithelial damage and associated bacterial translocation into the blood.

3.3. Case 3: presence of both TLR4 and TLR9

In Case 2, the effects of TLR4 but not TLR9 were included; as a result, the model tended to evolve toward disease outcomes, with a possibility of septic death and especially aseptic death due to uncontrolled inflammation. Several control mechanisms exist to prevent such tendencies from emerging under most circumstances. The action of enterocyte TLR9 is an example of such a control mechanism. In intestinal epithelial cells, it has been observed that

Author Manuscript Author Manuscript Author Manuscript Author Manuscript

the activation of TLR9 leads to the inhibition or dampening of TLR4 signaling (Sodhi et al., 2011).

In Case 3, the full model of six differential equations (Eqs. (1)–(7)) is used to simulate the interactions among bacteria, TLR4, TLR9, and the immune response. The effects of parameters $B_{M,source}$, k_{AD}, and a_1 on B_M and ε nullcline positions are similar to Cases 1 and 2; the overall effects of these parameters are summarized in Figs. 8 and 9.

In Fig. 8A, the $k_{AD} - B_{M,source}$ parameter space is divided into health, aseptic, and septic regions by curves representing Case 1 (blue), Case 2 (red), and Case 3 (black) with a_1 = 0.1/h. Simulating the model in the presence of both TLR4 and TLR9 transforms the previously aseptic region predicted in Case 2 to an entirely healthy region. In fact, even a small portion of the septic region predicted in Case 2 is predicted to be healthy when both TLR4 and TLR9 are included in the model (Case 3). This panel highlights the role of TLR9 in promoting homeostasis in a normal system, since TLR9 restores health in cases that were aseptic (points A and B) or septic (point C) in its absence.

In panels 8B–D, the time series for εB_M, ε, and R_E are shown for the parameter values that correspond to point B in Fig. 8A. Note that the combination of parameter values for point B correspond to septic death in Case 1, aseptic death in Case 2, and health in Case 3. In Fig. 8B, the time course of εB_M is shown relative to a dotted line that indicates the threshold value $T = 1.1 \times 10^6$ cells/g/h; in Fig. 8D, the time course of R_E is shown relative to a dotted line that indicates the TLR4 threshold value $T_{RE} = 0.65[R_E]$.

In Fig. 8B, the blue curve (Case 1) remains above the dotted T line, indicating that T is exceeded even at steady state and that bacteria are able to enter the blood. Permeability is also predicted to remain elevated for Case 1 (panel C). These combined results indicate a model prediction of septic death. TLR4 is absent in this case, and thus the blue curve corresponding to R_E is omitted in panel D. The red curves in these panels correspond to Case 2, with TLR4 present but TLR9 absent. In Fig. 8B, we see that $\varepsilon B_M < T$ and thus bacteria do not enter the blood/tissue. As observed in Fig. 8D, $R_E > T_{RE}$, which leads to increased inflammation, as evidenced by the elevated value of ε in panel C. From these panels, we observe that TLR4 molecules are able to keep B_M in check and keep εB_M below T, but since $P > 0$, $\varepsilon > \varepsilon_0$ and an aseptic death steady state is predicted.

The black curves in Fig. 8B–D represent Case 3, which includes both TLR4 and TLR9. In this case, TLR9 reins in TLR4 (and thus P) such that εB_M remains below T (Fig. 8B). As a result, B remains lower than it was previously and thus, after an elevated transient, R_E falls below T_{RE} (Fig. 8D). Since neither threshold is exceeded at steady state, bacteria are not present in the blood and $\varepsilon = \varepsilon_0$. This example shows that the addition of TLR9 brings the levels of activated TLR4 below the T_{RE} threshold, thereby reducing overall inflammation in the system and restoring health. A summary of the steady state outcomes at all three points labeled in Fig. 8A is provided in Table 3.

The $a_1 - B_{M,source}$ parameter space in Fig. 9 is divided into health, aseptic, and septic regions for Case 1 (blue), Case 2 (red), and Case 3 (black). The blue curve is vertical since TLR4 is absent in Case 1, and thus the resulting reduced model does not depend on a_1. The

Author Manuscript Author Manuscript Author Manuscript Author Manuscript

harmful effects of TLR4 are evident, particularly at high levels of TLR4 activation (high a_1) when a significant portion of the original health region (Case 1) is converted to aseptic death outcomes. Interestingly, for low a_1 values, there are regions of predicted septic death for Case 1 that become healthy in Case 2, even without TLR9, indicating an important role for TLR4 that was not obvious without running simulations in the presence and absence of the receptor. The addition of TLR9 (Case 3) reduces the degree of inflammation caused by TLR4 and expands the region where health is predicted. Even the inclusion of TLR9, however, cannot restore health in a part of the parameter region made aseptic by TLR4. Indeed, we see that even if parameters can be tuned so that the combined presence of TLR4 and TLR9 can be beneficial (e.g., $a_1 = 0.1$/h), there may be other parameter tunings such that their negative effects dominate (e.g., $a_1 \geq 0.2$/h), pointing to a possible mechanism for how an overactive TLR system can promote the emergence of NEC.

When both TLR4 and TLR9 are included in the model, TLR9 generally has beneficial effects; however, Point A in Fig. 9A represents an example of a situation in which the effects of TLR9 can be harmful (see also Fig. 10, where the same point is labeled, and especially Fig. 10B, which provides a zoomed view of the transition curves). Specifically, at Point A, the system is healthy in the presence of TLR4 (Case 2) but septic if TLR9 is included (Case 3). As can be seen more clearly from the temporal dynamics shown in Fig. 9B–D, this transition occurs when TLR9 inhibits TLR4 just enough so that the level of bacteria in the mucus becomes sufficiently high to cause the product of ε and B_M to exceed threshold (T). Bacteria can then enter the blood and invoke an immune response, causing R_E to increase above T_{RE} in Case 3; however, in this parameter regime, the TLR4 response in the presence of TLR9 is insufficient to combat the bacteria, and sepsis results.

The parameter space from Fig. 9A is duplicated in Fig. 10 and supplemented with an additional curve (green) that illustrates the effect of increasing k_{IE}, which is a key parameter promoting TLR9 activation. Increasing k_{IE} could correspond to administering a probiotic therapy or drug that favors TLR9 activation over TLR4 since probiotics are composed of a DNA sequence that is recognized by TLR9 receptors. Promoting TLR9 activation can restore aseptic regions to health (Cases 2 and 3) and also achieve healthy outcomes in a portion of the previously septic regions. The inset in panel B is included to highlight several parameter regimes in which the inclusion of TLR4, the inclusion of TLR4 and TLR9, or the enhancement of TLR9 via increased k_{IE} can lead to interesting effects. These outcomes are summarized in Table 4. Importantly, the correct balance of activation and inhibition of receptors and immune responses is necessary to maintain homeostasis and protect the host against infection, but this balance may depend on the severity of the bacterial invasion.

4. Discussion

TLR4 signaling contributes to the development of NEC by triggering increased inflammation and blocking processes such as proliferation and cell migration that are needed to repair the damaged epithelial layer (Sodhi et al., 2010; Leaphart et al., 2007). A model system of six ordinary differential equations is used in this study to simulate interactions among bacteria in the mucus layer, bacteria in the blood, the rate of bacterial translocation across the epithelium, pro-inflammatory cytokines, enterocyte TLR4, and enterocyte TLR9,

Author Manuscript Author Manuscript Author Manuscript Author Manuscript

with the goal of identifying how these interactions shape long-term health or disease outcomes. The data obtained in this study (Fig. 2) combined with additional experimental observations (Gribar et al., 2009; Sodhi et al., 2012) provide evidence for the central assumption underlying this model: an increase in TLR4 expression due to the presence of LPS can be attenuated by the response of TLR9 molecules to CpG DNA. While these data provide insight into the necessary mechanisms to include in a computational model, little data are available that would allow us to specify quantitative values for model parameters; therefore, we investigate the effects of varying several key parameters, building up from a model lacking TLR4 and TLR9, to a model including TLR4 alone, to a model with both types of TLR molecules included, to allow for the elucidation of specific contributions of each. Model results demonstrate a sensitive interplay among mucus layer dynamics, the severity of infection, and TLR activation. In particular, we showed how the relative promotion of health and disease by the combined TLR effects in the model depends on the rate of TLR4 activation by mucus layer bacteria. We also uncovered parameter regimes exhibiting unexpected outcomes, such as a direct promotion of health by TLR4 alone and the conversion of a state that is septic with TLR4 present into a healthy state by the inclusion of TLR9, which might not have been easily identified in an experimental setting. Fig. 3 gives a general summary of our findings, illustrating that TLR4 itself can promote health or disease, while the additional inclusion of TLR9 can promote health in place of disease, convert healthy states to disease, or maintain outcomes that occurred in its absence, depending on the balance of effects in the model.

Previous studies have established both deleterious and protective roles for TLR4 in the intestine (Sodhi et al., 2011). Our model is consistent with these observations, and its predictions of health or death are largely dependent on parameter values. For example, there are values of parameter a_1 (the parameter governing TLR4 activation) for which the presence of TLR4 alone can expand the health region and the additional inclusion of TLR9 further expands the predicted region of health. However, for large values of a_1, an aseptic death outcome may be predicted despite the combined effects of TLR4 and TLR9. We hypothesize that these effects of parameter values on system behavior could relate to the developmental status of the neonate in the context of NEC. For example, final maturation in the womb may bring about a balance of parameters that yields a healthy outcome whereas premature birth may correspond to a case of imbalanced parameters resulting in aseptic death despite the inhibitory effects of TLR9 on TLR4.

A “NEC scare” condition almost always precedes full-blown NEC and occurs if an infant’s bowel is suspected to be damaged. “NEC scare” infants or any infant that presents symptoms of NEC are managed with fluid resuscitation, total parenteral nutrition, bowel rest, and intravenous antibiotics (Petty and Ziegler, 2005). In many cases, there is no lasting damage to the bowel and no further treatment is needed. Although “NEC scare” is not explicitly addressed or defined in terms of model predictions, perhaps the point at which the threshold for bacterial translocation is first exceeded could be interpreted as the point at which an infant is expressing symptoms of “NEC scare”.

In full-blown cases of NEC, current therapy includes surgical resection of the necrotic area combined with supportive care for the infant (Guner et al., 2009) and is inadequate in many

Author Manuscript Author Manuscript Author Manuscript Author Manuscript

cases. Since surgical intervention for NEC is a very invasive procedure with a high rate of morbidity, computational studies can be used to explore possible effects of potential inflammation-modulating treatments for NEC. Here, several possible interventions are discussed in terms of key parameters affecting the system: reducing bacteria population in the lumen and mucus layer (parameter $B_{M,source}$), administering probiotic treatment or CpG DNA (parameter k_{IE}), and blocking TLR4 activation (parameter a_1). The model predicts that these interventions would be successful at restoring health in previously aseptic or septic steady state cases under most circumstances. However, the model is also used to show situations in which these interventions are not successful; a summary of these scenarios is provided in Table 5 and described in detail below for all three model cases considered. As a brief example, as stated in Table 5, the proposed treatment of decreasing $B_{M,source}$ would not be successful in Case 2 if a_1 is too high since inflammation becomes too high and aseptic death is predicted (justified by Fig. 7D). The results in Table 5 highlight the concept that testing of treatment strategies across multiple conditions is crucial when evaluating their potential effects.

4.1. Reducing bacterial population in lumen and mucus layer

Not surprisingly, in model Cases 1, 2, and 3, a decrease in the rate at which bacteria enter the mucus layer (defined here by parameter $B_{M,source}$) will almost always restore health. This effect can be seen, for example, from Figs. 7B and 8A, in which a decrease in the parameter $B_{M,source}$ causes any point in k_{AD}–$B_{M,source}$ parameter space to enter the healthy steady state region. However, there are important exceptions to consider. For example, values of parameters k_{PM} and a_1 can affect the health predictions in Case 1 and 2, respectively. If the rate of pro-inflammatory cytokine production due to blood/tissue bacteria condition (k_{PM}, Fig. 5D) or the rate of TLR4 activation by mucosal bacteria bowel is suspected to be damaged. (a_1, Fig. 7D) is elevated sufficiently, then $B_{M,source}$ must be extremely small to achieve a health outcome. It should be noted that $B_{M,source} = 0$ is not possible since there is always some degree of bacteria residing in the intestinal lumen after birth. While a low value of $B_{M,source}$ could correspond to treatment with antibiotics, antibiotics have not demonstrated efficacy in NEC since they increase TLR4 activation upon destroying bacterial components.

An intervention that could boost the host's ability to recognize and destroy foreign bacteria in the mucus layer (i.e., an increase in parameter k_{AD}) would have a similar effect on the system as decreasing $B_{M,source}$ (see Figs. 5A and 7A). Such an intervention may correspond to administering supplemental IgA. The low incidence of NEC among breastfed infants could relate to the immune bolstering effects of breast milk, whereas infants fed formula would be modeled using systems with lower k_{AD} values.

4.2. Administering probiotic treatment

Probiotic treatment in the context of NEC has been modeled previously (Arciero et al., 2010), and the effects of probiotics on NEC have been investigated in several experimental and clinical settings (Bin-Nun et al., 2005; Dani et al., 2002; Lin et al., 2008a; Fernandez-Carrocera et al., 2012; Mihatsch et al., 2012; Wang et al., 2012). Model predictions and experimental results have suggested that probiotics can decrease the incidence of NEC in the

Author Manuscript Author Manuscript Author Manuscript Author Manuscript

majority of cases but may trigger sepsis in a few situations. While these observations are encouraging, there is still insufficient evidence to recommend probiotics as a routine treatment for NEC (Mihatsch et al., 2012). Thus, the efficacy and safety of probiotics as a treatment for NEC should continue to be a subject of further study (AlFaleh et al., 2011), ideally with help from computational models.

Probiotic bacterial species often out-compete pathogenic bacteria in the lumen and help to restore the integrity of the epithelial barrier. Bacterial species contain a sequence of unmethylated DNA that is recognized differently from mammalian DNA; as a result, bacteria are identified and bound to certain receptors in the gut, such as TLR9 receptors, which in turn can inhibit TLR4. The effects of treatment with probiotics in Cases 1 and 2 would be similar to the effects of decreasing $B_{M,source}$, since probiotics are assumed to compete with pathogenic bacteria and decrease the rate at which bacteria enter the mucus layer. In Case 3, treatment with probiotics would also correspond to increasing parameter k_{IE}, since probiotics promote the activation of TLR9. As shown in Fig. 10, an increase in k_{IE} greatly increases the region of predicted health. However, in some instances, the model predicts that previously healthy cases become septic once k_{IE} is increased, demonstrating that probiotic treatments may be harmful in some cases. Point B in Fig. 10B represents an example of this outcome, where sufficient activation of TLR4 is required to keep B_M in check and thereby maintain $\varepsilon B_M < T$ and $B = 0$. An increase in a_1 could be used to boost TLR4 activation, but care would be needed to ensure that TLR9 activation is increased correspondingly to avoid aseptic death (e.g., switch from black to green in Fig. 10A). Although the conjectures about probiotics offered in this study do not specify probiotic type, it is important to note that different species of probiotics may have different effects in NEC. In addition, these probiotic effects most likely differ according to dosage, as observed in many clinical studies (Bin-Nun et al., 2005) and predicted by a previous mathematical model (Arciero et al., 2010). An important next step in utilizing this model will be the translation of the parameter values and regimes investigated mathematically into experimental and clinical terms to identify patient-specific cases in which probiotics should not be used as a treatment.

4.3. Blocking TLR4 activation

Experimental animal models have shown a significant reduction in the incidence of NEC when TLR4 is blocked; thus, administering an agent to block TLR4 activation is a potential therapeutic intervention for NEC. In the present model, TLR4 inhibition would correspond to decreasing the parameter a_1 to weaken TLR4 activation by mucosal bacteria. In Cases 2 and 3, a reduction in a_1 can convert an aseptic death outcome into a health steady state in many cases (Fig. 9). However, for larger $B_{M,source}$, the effects of altering a_1 are more subtle. For some values of $B_{M,source}$, reductions in a_1 can restore health in previously septic states since limiting inflammation preserves epithelial integrity and the corresponding influx of bacteria into the blood/tissue. With further reductions of a_1, however, sepsis still results (e.g., near point A in Fig. 9A), due to an insufficient ability to eliminate bacteria. This effect may relate to the reason that TLR4 has been conserved evolutionarily and been thought to play a protective role in non-newborn states (Afrazi et al., 2011). Finally, for some levels of

Author Manuscript Author Manuscript Author Manuscript Author Manuscript

infection (corresponding to very high $B_{M,source}$), septic death is predicted regardless of whether or not TLR4 is blocked.

4.4. Concluding remarks

Tables 3–5 and Fig. 10 show the importance of obtaining an appropriate balance among the various immune response defense mechanisms. For example, preventing excessive entry of bacteria into the mucus layer is necessary to avoid an overly robust inflammatory response to commensal bacteria. Given the presence of mucus layer bacteria, bacterial destruction by intestinal macrophages (represented by the threshold T in the model) is also necessary to prevent bacteria from entering the intestinal tissue or systemic circulation. Finally, the body must be able to respond in an adequately robust, appropriate fashion to infections when the epithelial barrier is breached. However, the degree of inflammation must be regulated so that the body does not enter a continually inflamed, self-maintaining state (Vodovotz et al., 2008, 2009; An et al., 2012); in terms of our model, activated TLR4 must decrease below T_{RE} at some point in time to achieve a healthy outcome. The model presented in this study is used to describe cases in which these immune mechanisms work at an appropriate or inappropriate level, leading to various outcomes for the system. As part of this description, we have highlighted roles of particular system components in achieving healthy outcomes and ways that they can become unbalanced, resulting in detrimental effects.

Some of the regions predicted in the model are small and perhaps difficult to realize since they represent a very specific combination of parameter values. However, NEC is a disease that only affects a very small percentage of the premature infant population and thus, the question of what dictates whether an infant develops NEC may be related to the regimes identified in the model. More tightly linking model parameters to specific biological effects and using additional experiments to constrain the values of these parameters would be useful in undertaking a more quantitative investigation of the mechanisms that give rise to NEC.

Intestinal macrophages are an important mechanism of defense by which the immune system responds to an invading pathogen. As described earlier, instead of explicitly tracking the population of macrophages in the enterocyte in this model, we set a numerical threshold to take into account their effects on bacterial translocation from lumen to blood/tissue. This threshold value can be increased or decreased to simulate a system in which intestinal macrophages are more or less capable of eliminating bacteria in the mucus layer. Experimental studies have identified a different expression and activity of TLR4 and TLR9 in macrophages than in enterocytes (Gribar et al., 2009); including TLR4 and TLR9 populations associated with intestinal macrophages in a future model may provide additional insight into the pathogenesis of NEC. Expanding the model to include additional inflammatory mechanisms and explicit tissue damage may also help to unravel which responses or mechanisms contribute most significantly to NEC.

The current model is developed in the context of a premature infant. However, the model could be adapted to answer questions about both premature infants and full term infants by assigning different parameters to each population. For example, the baseline rate of bacterial translocation may be greater in premature infants than full term infants due to the immaturity of the intestinal layer. Similarly, the immune response of a premature infant is less selective

Author Manuscript Author Manuscript Author Manuscript Author Manuscript

than that of a full term infant, which also exhibits more mechanisms of negative regulation to prevent chronic inflammation. Using and adapting the model to compare these two populations may help in better understanding the factors contributing to NEC and other chronic intestinal diseases.

Acknowledgments

This work was partially supported by National Science Foundation Award EMSW21-RTG 0739261.

References

Afrazi A, Sodhi C, Richardson W, Neal M, Good M, Siggers R, Hackam D. New insights into the pathogenesis and treatment of necrotizing enterocolitis: Toll-like receptors and beyond. Pediatr. Res. 2011; 69(3):183–187. [PubMed: 21135755]

Akira S, Takeda K, Kaisho T. Toll-like receptors: critical proteins linking innate and acquired immunity. Nat. Immunol. 2001; 2(8):675–680. [PubMed: 11477402]

AlFaleh K, Anabrees J, Bassler D, Al-Kharfi T. Probiotics for prevention of necrotizing enterocolitis in preterm infants. Cochrane Database Syst. Rev. 2011; 3 (CD005496), http://dx.doi.org/10.1002/14651858.CD005496.pub3.

An G, Nieman G, Vodovotz Y. Computational and systems biology in trauma and sepsis: current state and future prospects. Int. J. Burns Trauma. 2012; 2:1–10. [PubMed: 22928162]

Arciero J, Ermentrout G, Upperman J, Vodovotz Y, Rubin J. Using a mathematical model to analyze the role of probiotics and inflammation in necrotizing enterocolitis. PLoS ONE. 2010; 5(4):e10066. http://dx.doi.org/10.1371/journal.pone.0010066. [PubMed: 20419099]

Bianchi M, Manfredi A. Dangers in and out. Science. 2009; 323:1683–1684. [PubMed: 19325105]

Bin-Nun A, Bromiker R, Wilschanski M, Kaplan M, Rudensky B, Caplan M, Hammerman C. Oral probiotics prevent necrotizing enterocolitis in very low birth weight neonates. J. Pediatr. 2005; 147(2):192–196. [PubMed: 16126048]

Chan K, Wong K, Luk J. Role of LPS-CD14-TLR4-mediated inflammation in necrotizing enterocolitis: pathogenesis and therapeutic implications. World J. Gastroenterol. 2009; 15(38): 4745–4752. [PubMed: 19824106]

Claud E, Lu L, Anton P, Savidge T, Walker W, Cherayil B. Developmentally regulated I-kappaB expression in intestinal epithelium and susceptibility to flagellin-induce inflammation. Proc. Natl. Acad. Sci. USA. 2004; 101(19):7404–7408. [PubMed: 15123821]

Collado M, Cernada M, Bauer C, Vento M, Perez-Martinez G. Microbial ecology and host–microbiota interactions during early life stages. Gut Microbes. 2012; 3(4):352–365. [PubMed: 22743759]

Corazziari E. Intestinal mucus barrier in normal and inflamed colon. J. Pediatr. Gastroenterol. Nutr. 2009; 48:S54–S55. [PubMed: 19300126]

Dani C, Biadaioli R, Bertini G, Martelli E, Rubaltelli F. Probiotics feeding in prevention of urinary tract infection, bacterial sepsis and necrotizing enterocolitis in preterm infants. A prospective double-blind study. Biol. Neonate. 2002; 82(2):103–108. [PubMed: 12169832]

Deitch E. Simple intestinal obstruction causes bacterial translocation in man. Arch. Surg. 1989; 124:699–701. [PubMed: 2730322]

Deitch E. Role of bacterial translocation in necrotizing enterocolitis. Acta Pediatr. 1994; 396:33–36.

Duerkop B, Vaishnava S, Hooper L. Immune responses to the microbiota at the intestinal mucosal surface. Immunity. 2009; 31:368–376. [PubMed: 19766080]

Edde L, Hipolito R, Hwang F, Headon D, Shalwitz R, Sherman M. Lactoferrin protects neonatal rats from gut-related systemic infection. Am. J. Physiol. Gastrointest. Liver Physiol. 2001; 281:1140–1150.

Edelson M, Bagwell C, Rozycki H. Circulating pro- and counter inflammatory cytokine levels and severity in necrotizing enterocolitis. Pediatrics. 1999; 103(4):766–771. [PubMed: 10103300]

Fernandez-Carrocera L, Solis-Herrera A, Cabanillas-Ayon M, Gallardo-Sarmiento R, Garcia-Perez C, Montano-Rodriguez R, Echaniz-Aviles M. Double-blind, randomised clinical assay to evaluate the

Author Manuscript Author Manuscript Author Manuscript Author Manuscript

efficacy of probiotics in preterm newborns weighing less than 1500 g in the prevention of necrotising enterocolitis. Arch. Dis. Child Fetal Neonatal Ed. 2012 http://dx.doi.org/10.1136/archdischild-2011-300435.

Gregory K, DeForge C, Natale K, Phillips M, VanMarter L. Necrotizing enterocolitis in the premature infant. Adv. Neonatal Care. 2011; 11(3):155–164. [PubMed: 21730907]

Gribar S, Sodhi C, Richardson W, Anand R, Gittes G, Branca M, Jakub A, Shi X, Shah S, Ozolek J, Hackam D. Reciprocal expression and signaling of TLR4 and TLR9 in the pathogenesis and treatment of necrotizing enterocolitis. J. Immunol. 2009; 182:636–646. [PubMed: 19109197]

Guner Y, Friedlich P, Wee C, Dorey F, Camerini V, Upperman J. State-based analysis of necrotizing enterocolitis outcomes. J. Surg. Res. 2009; 157:21–29. [PubMed: 19615694]

Hackam D, Upperman J, Grishin A, Ford H. Disordered enterocyte signaling and intestinal barrier dysfunction in the pathogenesis of necrotizing enterocolitis. Semin. Pediatr. Surg. 2005; 14:49–57. [PubMed: 15770588]

Haller D, Bode C, Hammes W, Pfeifer A, Schiffrin E, Blum S. Non-pathogenic bacteria elicit a differential cytokine response by intestinal epithelial cell/leucocyte co-cultures. Gut. 2000; 47:79–87. [PubMed: 10861268]

Han X, Fink M, Yang R, Delude R. Increased iNOS activity is essential for intestinal epithelial tight junction dysfunction in endotoxemic mice. Shock. 2004; 21(3):261–270. [PubMed: 14770040]

Harris M, Costarino A, Sullivan J, Dulkerlan S, McCawley L, Corcoran L, Butler S, Kilpatrick L. Cytokine elevations in critically ill infants with sepsis and necrotizing enterocolitis. J. Pediatr. 1994; 124:105–111. [PubMed: 8283358]

Hecht G. Innate mechanisms of epithelial host defense: spotlight on intestine. Am. J. Physiol. Cell Physiol. 1999; 277:351–358.

Hooper L, Macpherson A. Immune adaptations that maintain homeostasis with the intestinal microbiota. Nat. Rev. Immunol. 2010; 10:159–169. [PubMed: 20182457]

Hunter C, Upperman J, Ford H, Camerini V. Understanding the susceptibility of the premature infant to necrotizing enterocolitis (NEC). Pediatr. Res. 2008; 63(2):117–123. [PubMed: 18091350]

Ivory C, Prystajecky M, Jobin C, Chadee K. Toll-like receptor 9-dependent macrophage activation by entamoeba histolytica DNA. Inf. Immun. 2008; 76(1):289–297.

Kim M, Christley S, Alverdy J, Liu D, An G. Immature oxidative stress management as a unifying principle in the pathogenesis of necrotizing enterocolitis: insights from an agent-based model. Surg. Inf. 2012; 13(1) http://dx.doi.org/10.1089/sur.2011.057.

Kubinak J, Round J. Toll-like receptors promote mutually beneficial commensal–host interactions. PLoS Pathogens. 2012; 8(7):e1002785. http://dx.doi.org/10.1371/journal.ppat.1002785. [PubMed: 22910541]

Lan J, Cruickshank S, Sing J, Farrar M, Lodge J, Felsburg P, Carding S. Different cytokine response of primary colonic epithelial cells to commensal bacteria. World J. Gastroenterol. 2005; 11(22): 3375–3384. [PubMed: 15948242]

Leaphart C, Cavallo J, Gribar S, Cetin S, Li J, Branca M, Dubowski T, Sodhi C, Hackam D. A critical role for TLR4 in the pathogenesis of necrotizing enterocolitis by modulating intestinal injury and repair. J. Immunol. 2007; 179:4808–4820. [PubMed: 17878380]

Leser T, Molbak L. Better living through microbial action: the benefits of the mammalian gastrointestinal microbiota on the host. Environ. Microbiol. 2009; 11(9):2194–2206. [PubMed: 19737302]

Lin H, Hsu C, Chen H, Chung M, Hsu J, Lien R, Tsao L, Chen C, Su B. Oral probiotics prevent necrotizing enterocolitis in very low birth weight preterm infants: a multicenter randomized controlled trial. Pediatrics. 2008a; 122(4):693–700. [PubMed: 18829790]

Lin P, Nasr T, Stoll B. Necrotizing enterocolitis: recent scientific advances in pathophysiology and prevention. Semin. Perinatol. 2008b; 32(2):70–82. [PubMed: 18346530]

Liu Y, Zhu L, Fatheree N, Liu X, Pacheco S, Tatevian N, Rhoads J. Changes in intestinal Toll-like receptors and cytokines precede histological injury in a rat model of necrotizing enterocolitis. Gastroenterology. 2009; 297:G442–G450.

Lotz M, Gutle D, Walther S, Menard S, Bogdan C, Hornef M. Postnatal acquisition of endotoxin tolerance in intestinal epithelial cells. J. Exp. Med. 2006; 203(4):973–984. [PubMed: 16606665]

Author Manuscript Author Manuscript Author Manuscript Author Manuscript

Maheshwari A, Kelly D, Nicola T, Ambalavanan N, Jain S, Murphy-Ullrich J, Athar M, Shimamura M, Bhandari V, Aprahamian C, Dimmitt R, Serra R, Ohls R. TGF-beta2 suppresses macrophage cytokine production and mucosal inflammatory responses in the developing intestine. Gastroenterology. 2011; 140(1):242–253. [PubMed: 20875417]

Meyer-Hoffert U, Hornef M, Henriques-Normark B, Axelsson L, Midtvedt T, Putsep K, Anderson M. Secreted enteric antimicrobial activity localises to the mucus surface layer. Gut. 2008; 57:764–771. [PubMed: 18250125]

Mihatsch W, Braegger C, Decsi T, Kolacek S, Lanzinger H, Mayer B, Moreno L, Pohlandt F, Puntis J, Shamir R, Stadtmuller U, Szajewska H, Turck D, vanGoudoever J. Critical systematic review of the level of evidence for routine use of probiotics for reduction of mortality and prevention of necrotizing enterocolitis and sepsis in preterm infants. Clin. Nutr. 2012; 31:6–15. [PubMed: 21996513]

Neal M, Leaphart C, Levy R, Prince J, Billiar T, Watkins W, Li J, Cetin S, Ford H, Schreiber A, Hackam D. Enterocyte TLR4 mediates phagocytosis and translocation of bacteria across the intestinal barrier. J. Immunol. 2006; 176:3070–3079. [PubMed: 16493066]

Neish A, Gewirtz A, Zeng H, Young A, Hobert M, Karmali V, Rao A, Madara J. Prokaryotic regulation by epithelial responses by inhibition of IkB-alpha ubiquitination. Science. 2000; 289:1560–1563. [PubMed: 10968793]

Ohland C, MacNaughton W. Probiotic bacteria and intestinal epithelial barrier function. Am. J. Physiol. Gastrointest. Liver Physiol. 2010; 298:G807–G819. [PubMed: 20299599]

Papoff P, Ceccarelli G, d'Ettore G. Gut microbial translocation in critically ill children and effects of supplementation with pre- and probiotics. Int. J. Microbiol. 2012 http://dx.doi.org/10.1155/2012/151393.

Petty J, Ziegler M. Operative strategies for necrotizing enterocolitis: the prevention and treatment of short-bowel syndrome. Semin. Pediatr. Surg. 2005; 14(3):191–198. [PubMed: 16084407]

Qureshi F, Leaphart C, Cetin S, Li J, Grishin A, Watkins S, Ford H, Hackam D. Increased expression and function of integrins in enterocytes by endotoxin impairs epithelial restitution. Gastroenterology. 2005; 128:1012–1022. [PubMed: 15825082]

Rakoff-Nahoum S, Paglino J, Eslami-Varzaneh F, Edberg S, Medzhitov R. Recognition of commensal microflora by Toll-like receptors is required for intestinal homeostasis. Cell. 2004; 118:229–241. [PubMed: 15260992]

Reynolds A, Rubin J, Clermont G, Day J, Vodovotz Y, Ermentrout G. A reduced mathematical model of the acute inflammatory response: I derivation of model and analysis of anti-inflammation. J. Theor. Biol. 2006; 242:220–236. [PubMed: 16584750]

Samel S, Keese M, Kleczka M, Lanig S, Gretz N, Hafner M, Sturm J, Post S. Microscopy of bacterial translocation during small bowel obstruction and ischemia in vivo – a new animal model. BMC Surg. 2002; 2

Sherman M. New concepts of microbial translocation in the neonatal intestine: mechanisms and prevention. Clin. Perinatol. 2010; 37(3):565–579. [PubMed: 20813271]

Smith P, Ochsenbauer-Jambor C, Smythies L. Intestinal macrophages: unique effector cells of the innate immune system. Immunol. Rev. 2005; 206:149–159. [PubMed: 16048547]

Smythies L, Sellers M, Clements R, Mosteller-Barnum M, Meng G, Benjamin W, Orenstein J, Smith P. Human intestinal macrophages display profound inflammatory anergy despite avid phagocytic and bacteriocidal activity. J. Clin. Invest. 2005; 115(1):66–75. [PubMed: 15630445]

Sodhi C, Levy R, Gill R, Neal M, Richardson W, Branca M, Russo A, Prindle T, Billiar T, Hackam D. DNA attenuates enterocyte Toll-like receptor 4-mediated intestinal mucosal injury after remote trauma. Am. J. Physiol. Gastrointest. Liver Physiol. 2011; 300:G862–G873. [PubMed: 21233273]

Sodhi C, Neal M, Siggers R, Sho S, Ma C, Branca M, Prindle T Jr, Russo A, Afraz A, Good M, Brower-Sinning R, Firek B, Morowitz M, Ozolek J, Gittes G, Billiar T, Hackam D. Intestinal epithelial Toll-like receptor 4 regulates goblet cell development and is required for necrotizing enterocolitis in mice. Gastroenterology. 2012; 2143:708–718. [PubMed: 22796522]

Sodhi C, Shi X, Richardson W, Grant Z, Shapiro R, Prindle T Jr, Branca M, Russo A, Gribar S, Congrong M, Hackam D. Toll-like receptor-4 inhibits enterocyte proliferation via impaired β-

Author Manuscript Author Manuscript Author Manuscript Author Manuscript

catenin signaling in necrotizing enterocolitis. Gastroenterology. 2010; 138:185–196. [PubMed: 19786028]

Turroni F, Peano C, Pass D, Foroni E, et al. Diversity of bifidobacteria within the infant gut microbiota. PLoS ONE. 2012; 7(5):e36957. http://dx.doi.org/10.1371/journal.pone.0036957. [PubMed: 22606315]

Vaishnava S, Behrendt C, Ismail A, Eckmann L, Hooper L. Paneth cells directly sense gut commensals and maintain homeostasis at the intestinal host–microbial interface. Proc. Natl. Acad. Sci. USA. 2008; 105(52):20858–20863. [PubMed: 19075245]

Vodovotz Y, Constantine G, Rubin J, Csete M, Voit E, An G. Mechanistic simulations of inflammation: current state and future prospects. Math. Biosci. 2009; 217:1–10. [PubMed: 18835282]

Vodovotz Y, Csete M, Bartels J, Chang S, An G. Translational systems biology of inflammation. PLoS Comput. Biol. 2008; 4:1–6.

Wang Q, Dong J, Zhu Y. Probiotic supplement reduces risk of necrotizing enterocolitis and mortality in preterm very low-birth-weight infants: an updated meta-analysis of 20 randomized, controlled trials. J. Pediatr. Surg. 2012; 47:241–248. [PubMed: 22244424]

Wenzl H, Schimpl G, Feierl G, Steinwender G. Time course of spontaneous bacterial translocation from gastrointestinal tract and its relationship to intestinal microflora in conventionally reared infant rats. Dig. Dis. Sci. 2001; 46(5):1120–1126. [PubMed: 11341658]

Xavier R, Podolsky D. How to get along—friendly microbes in a hostile world. Science. 2000; 289:1483–1484. [PubMed: 10991734]

Author Manuscript Author Manuscript Author Manuscript Author Manuscript

HIGHLIGHTS

- A mathematical model assesses the role of inflammation in necrotizing enterocolitis.
- The model demonstrates how bacteria–immune interactions can affect health outcomes.
- The model predicts a sensitive interplay between bacteria and receptor activation.
- The model identifies unexpected disease outcomes not easily detected by experiments.
- The model evaluates whether potential NEC treatment strategies could be effective.

Author Manuscript Author Manuscript Author Manuscript Author Manuscript

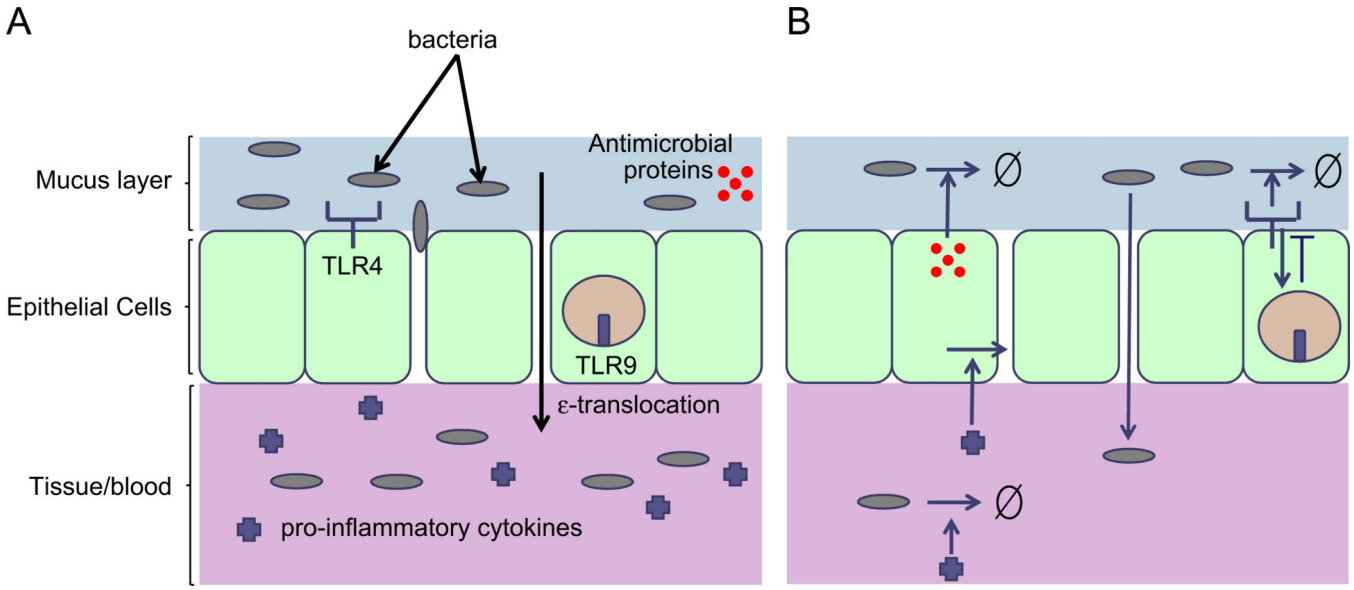

Fig. 1.

A. Schematic of model (not to scale). B. Interactions of bacteria and the immune response in NEC are described using a compartmental model of the small intestine. Bacteria (gray) enter the mucus layer where they are recognized by enterocyte TLR4 (labeled) or dendritic cells and may be eliminated by antimicrobial proteins (red). Enterocyte TLR9 (labeled) activation inhibits TLR4 signaling, whereas enterocyte TLR4 activation triggers TLR9 signaling. Bacterial translocation (ε) across the intestinal epithelium (green) occurs via gaps in the layer or internalization. Pro-inflammatory cytokine (+) production is triggered in the lumped blood/tissue compartment (purple) if bacteria breach the epithelial barrier. The pro-inflammatory cytokines trigger the elimination of bacteria in the blood but also cause damage to the epithelial layer, promoting an increased rate of bacterial translocation. (For interpretation of the references to color in this figure caption, the reader is referred to the web version of this paper.)

Author Manuscript Author Manuscript Author Manuscript Author Manuscript

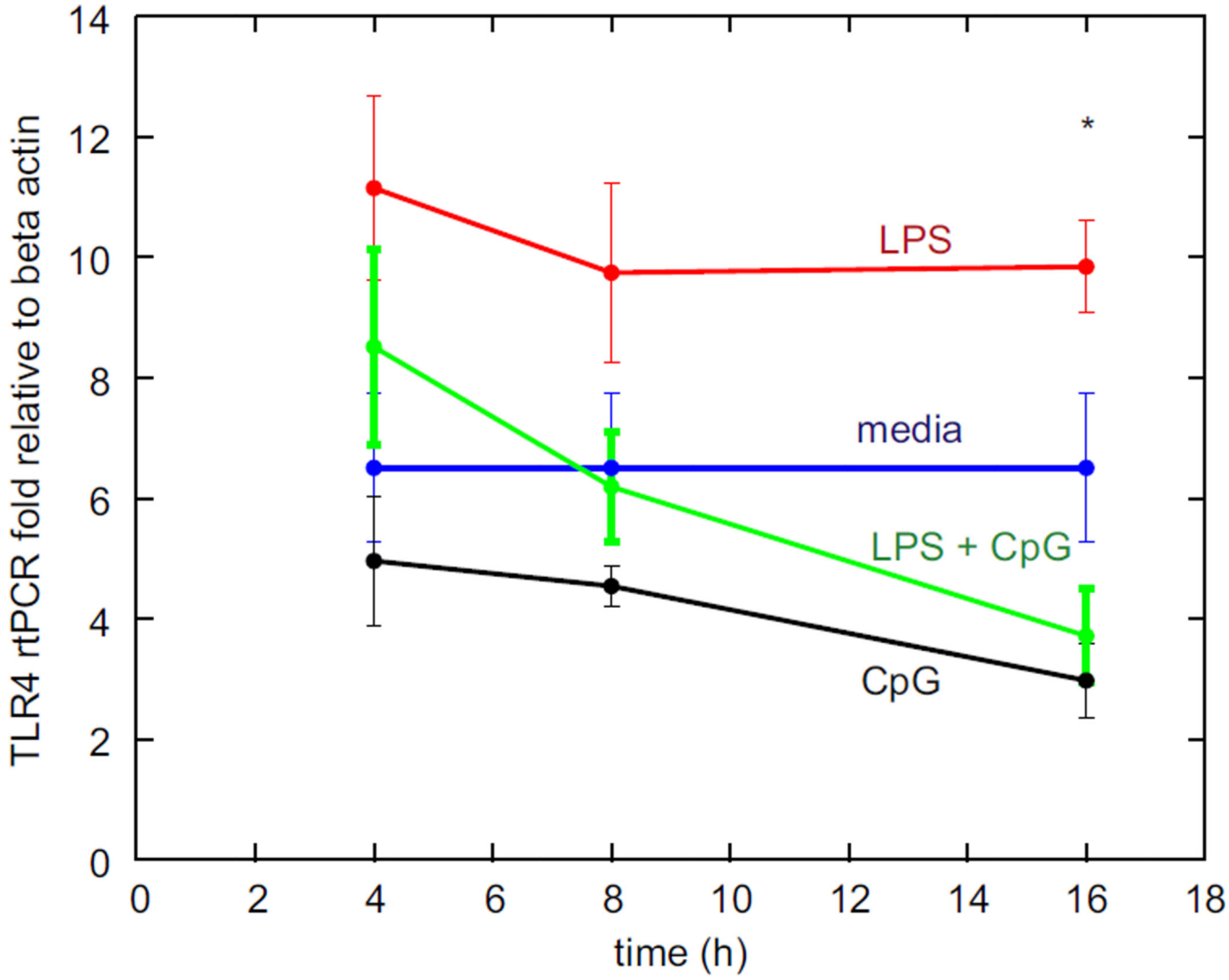

Fig. 2.

TLR4 expression on IEC6 enterocytes at 4, 8, and 16 h. All values are compared with control state (media, blue). TLR4 expression increases if LPS (red) is added to the system. TLR4 expression is decreased in the presence of CpG DNA (black). When both LPS and CpG DNA (green) are added to the system, the TLR4 expression decreases with time. The * denotes a statistically significant difference in TLR4 expression between LPS and LPS + CpG data groups at 16 h ($p < 0.05$). (For interpretation of the references to color in this figure caption, the reader is referred to the web version of this paper.)

Author Manuscript Author Manuscript Author Manuscript Author Manuscript

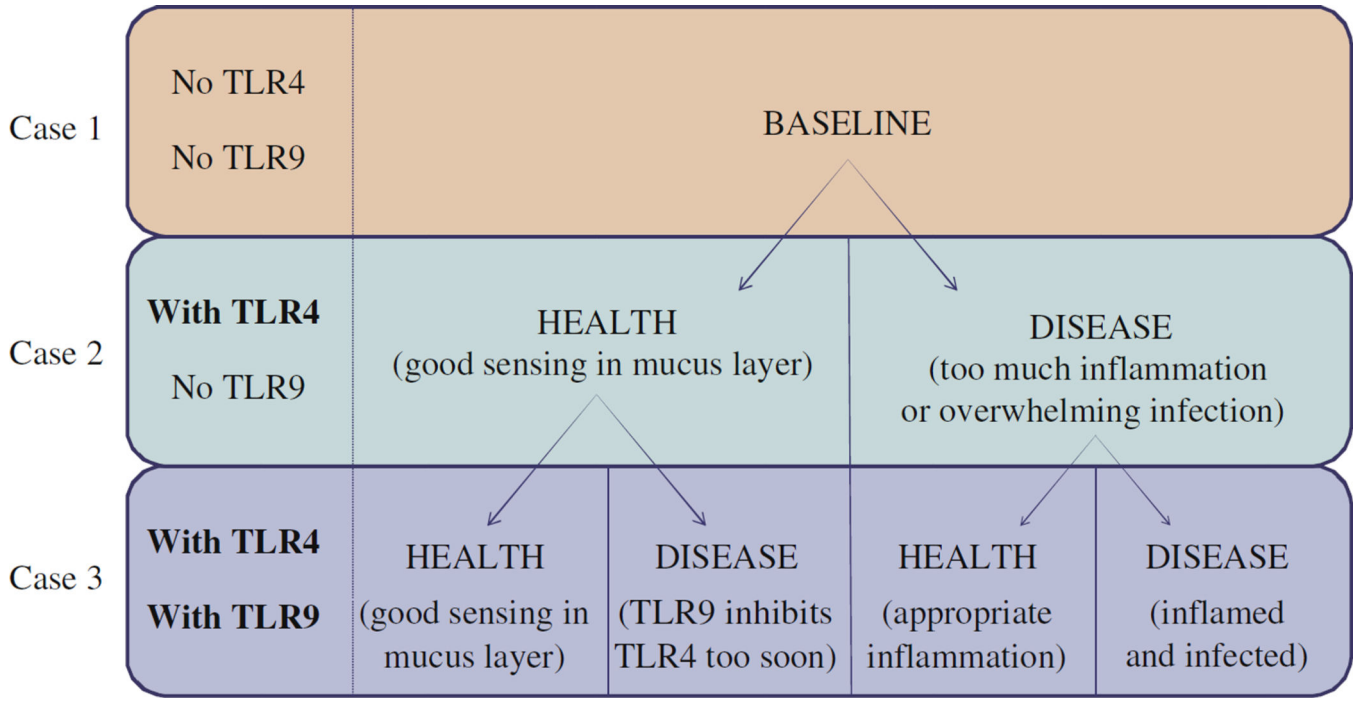

Fig. 3.

Description of the three cases, or levels of model complexity, presented in this work and summary of the outcomes that may result. Case 1: no TLR4 and no TLR9 are present in the model. Whichever outcome, health or disease, occurs is considered a baseline result, which may possibly be modified by the inclusion of TLR4 or TLR4 plus TLR9. Case 2: with TLR4 but no TLR9. A health state can be achieved if TLR4 activation leads to sufficient bacterial killing at the mucus layer level but does not lead to overwhelming inflammation; otherwise, a disease state results. Case 3: with TLR4 and with TLR9. Addition of TLR9 helps to lessen harmful effects of TLR4, and thus promotes health, in some scenarios, but may suppress its positive effects, and thus induce disease, in others.

Author Manuscript Author Manuscript Author Manuscript Author Manuscript

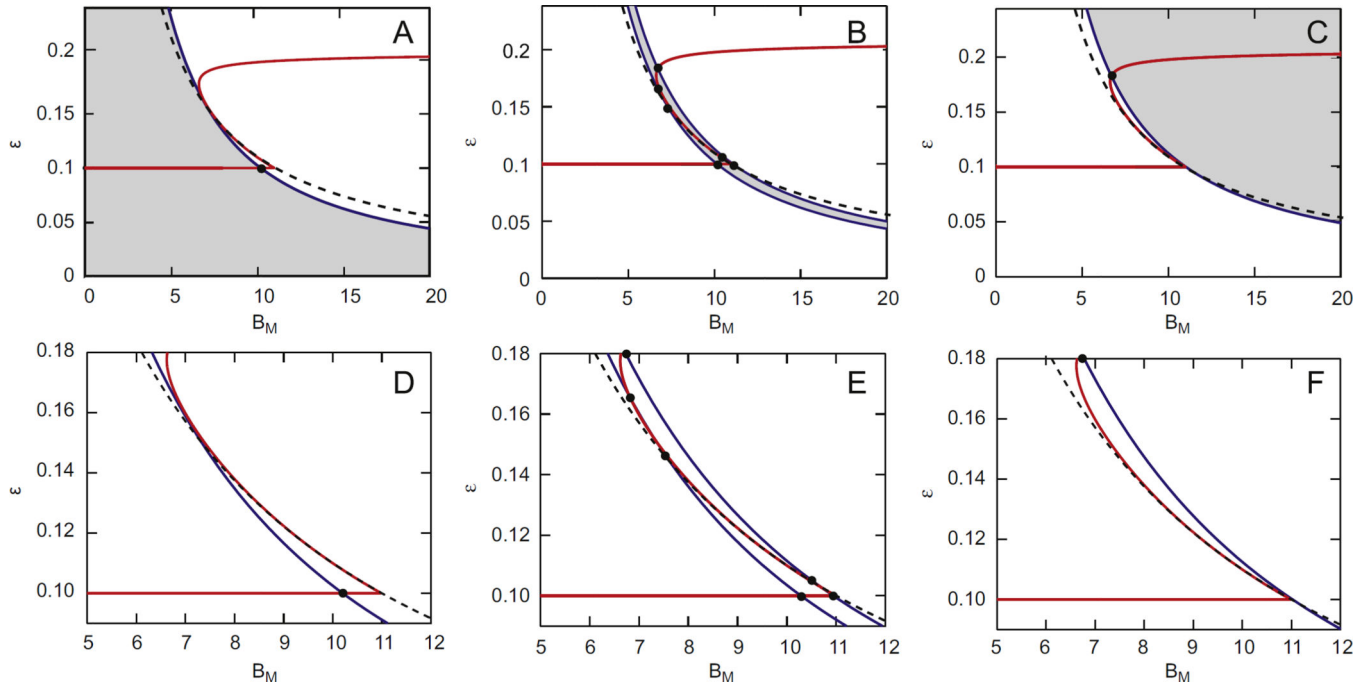

Fig. 4.

Dynamics for Case 1 displayed in the ε−B_M phaseplane. $R_E = I_E \equiv 0$. Red curves: ε nullcline ($d\varepsilon/dt = 0$). Blue curves: B_M nullcline ($dB_M/dt = 0$). Dotted black curves: $\varepsilon B_M = T$. In each panel, $k_{AD} = 1$. A. Shaded region corresponds to locations of B_M nullcline for 0×10^6 cells/g/h ≤ $B_{M,source} \leq 1.65 \times 10^6$ cells/g/h, such that the B_M and ε nullclines intersect at a healthy steady state. B. Shaded region corresponds to locations of B_M nullcine yielding a bistable regime in which a health or disease steady state is predicted depending on $B_M(0)$. Bistability occurs for 1.66×10^6 cells/g/h ≤ $B_{M,source} \leq 1.74 \times 10^6$ cells/g/h. C. Shaded region corresponds to locations of B_M nullclines yielding a single disease steady state, as arises for $B_{M,source} \geq 1.75 \times 10^6$ cells/g/h. D–F. Zoomed versions of panels A–C to clearly show nullcline and threshold intersections. (For interpretation of the references to color in this figure caption, the reader is referred to the web version of this paper.)

Author Manuscript Author Manuscript Author Manuscript Author Manuscript

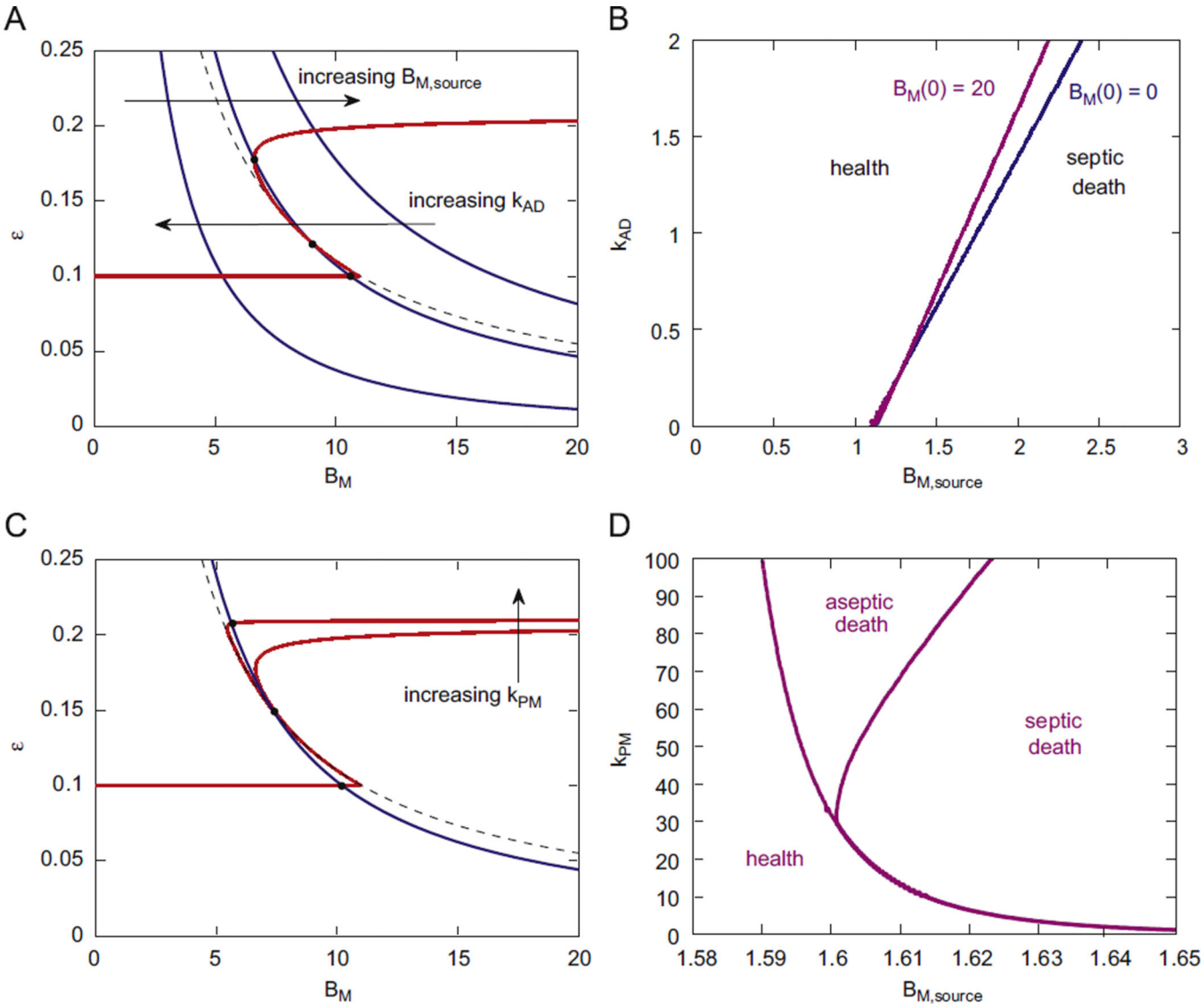

Fig. 5.

Dynamics for Case 1 as parameters $B_{M,source}$, k_{AD}, and k_{PM} are varied. A. ε−B_M phase plane with varied $B_{M,source}$ and k_{AD}. The B_M nullcline shifts rightward as $B_{M,source}$ is increased or k_{AD} is decreased. This shows that altering the rate of bacterial entry into the mucus layer or the rate of bacterial killing by dendritic cells can change the stability of the steady state. B. A summary of health and disease steady states are given in k_{AD}−$B_{M,source}$ parameter space. Combinations of parameter values to the left of the curves indicate healthy steady states and points to the right of the curve are septic death steady states. Two initial conditions are shown: $B_M(0) = 0 \times 10^6$ cells/g/h (blue) and $B_M(0) = 20 \times 10^6$ cells/g/h (magenta). Bistability is predicted in the region between the blue and magenta curves. C. ε −B_M phase plane with varied k_{PM}. As more pro-inflammatory cytokines are activated (i.e., parameter k_{PM} is increased), there is a shift in the ε nullcline and the position and classification of equilibrium points. D. Summary of health and disease steady states in the k_{PM}−$B_{M,source}$ parameter space for $B_M(0) = 20 \times 10^6$ cells/g/h. The entire parameter space

Author Manuscript Author Manuscript Author Manuscript Author Manuscript

(for the depicted ranges of parameter values) yields a health outcome if $B_M(0) = 0 \times 10^6$ cells/g/h (not shown). In panels C and D, $k_{AD} = 1 \times 10^6$ cells/g/h. (For interpretation of the references to color in this figure caption, the reader is referred to the web version of this paper.)

Author Manuscript Author Manuscript Author Manuscript Author Manuscript

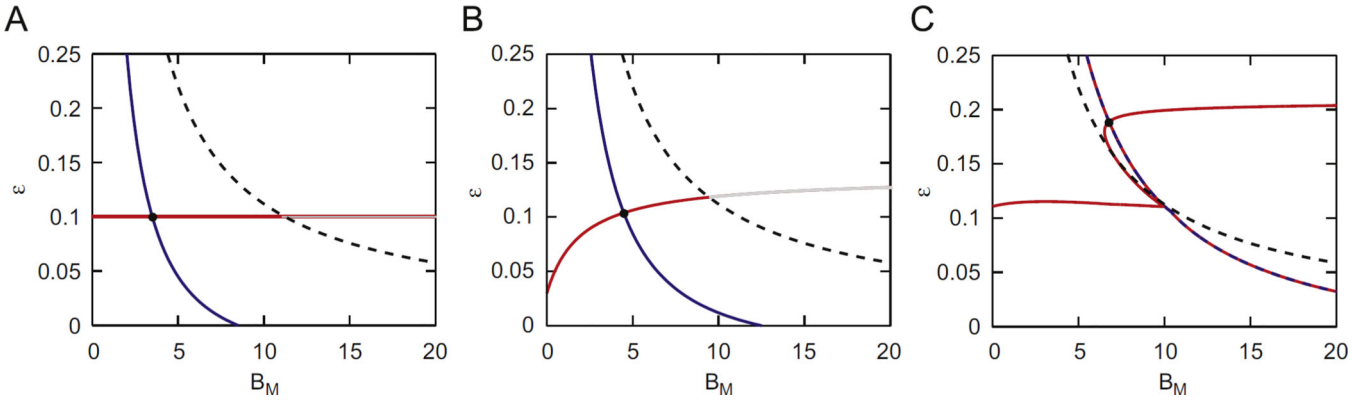

Fig. 6.

Dynamics for Case 2, which includes TLR4 but not TLR9 (i.e., $I_E \equiv 0$), displayed in the $\varepsilon - B_M$ phaseplane. Red curves: ε nullcline ($d\varepsilon/dt = 0$). Blue curves: B_M nullcline ($dB_M/dt = 0$). Dotted black curves: $\varepsilon B_M = T$. A. Nullclines are shown for the case when $\varepsilon B_M < T$ and $R_E < T_{RE}$. A healthy equilibrium point is predicted. B. Nullclines are shown for $\varepsilon B_M < T$ and $R_E > T_{RE}$. An aseptic death steady state is predicted. In panels A and B, the grey portion of the ε nullclines indicate regions that are inconsistent with the assumption $\varepsilon B_M < T$. C. Nullclines are shown for the case when $\varepsilon B_M > T$ and $R_E > T_{RE}$. A septic death steady state is predicted. (For interpretation of the references to color in this figure caption, the reader is referred to the web version of this paper.)

Author Manuscript Author Manuscript Author Manuscript Author Manuscript

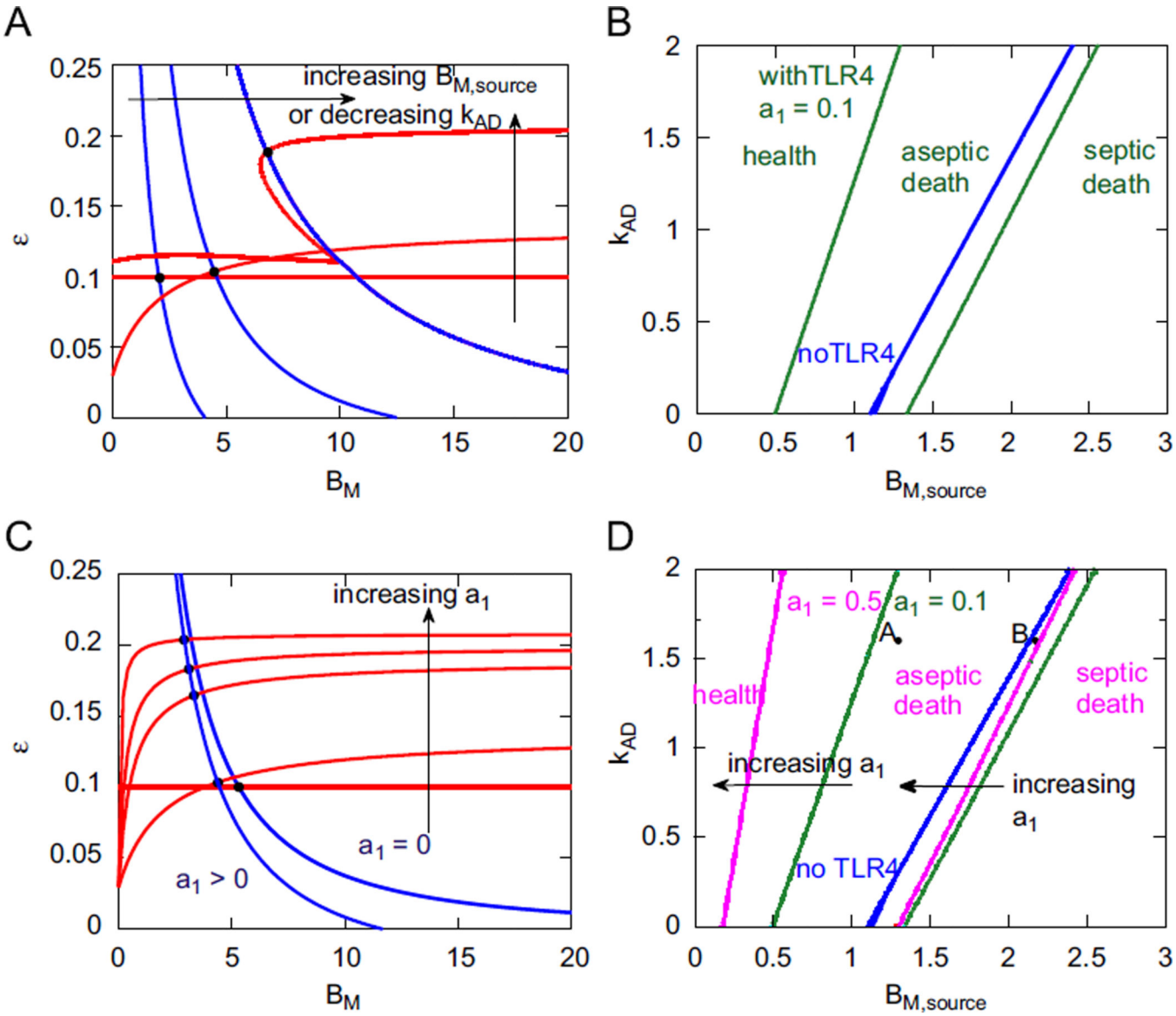

Fig. 7.

Dynamics for Case 2, which includes TLR4 but not TLR9, with parameters $B_{M,source}$, k_{AD}, and a_1 varied. A. ε−B_M phase plane with $B_{M,source}$ or k_{AD} varied. The B_M nullcline shifts rightward as $B_{M,source}$ is increased or k_{AD} is decreased (with a_1 = 0.1/h). The ε nullcline also changes shape or slope with changes in $B_{M,source}$ and k_{AD}. B. Summary of health and disease steady states in k_{AD}−$B_{M,source}$ parameter space (as in Fig. 5). Summary is provided for Case 1 (blue) and Case 2 (green) when a_1 = 0.1/h. C. ε−B_M phase plane with parameter a_1 varied (k_{AD} = 1 × 10^6 cells/g/h and $B_{M,source}$ = 1.6 × 10^6 cells/g/h). As TLR4 activation increases (increase in parameter a_1), there is an upward shift of the ε nullcline. D. Summary of health and disease steady states are given in k_{AD}−$B_{M,source}$ parameter space for a_1 = 0/h (blue), 0.1/h (green), and 0.5/h (magenta). Point A is an example of a steady state that is predicted to be healthy in Case 1 but that is predicted to be aseptic when the effects of TLR4 are considered (Case 2). Point B is an example of a septic steady state (Case 1) that becomes

aseptic in Case 2. (For interpretation of the references to color in this figure caption, the reader is referred to the web version of this paper.)

Author Manuscript Author Manuscript Author Manuscript Author Manuscript

Author Manuscript Author Manuscript Author Manuscript Author Manuscript

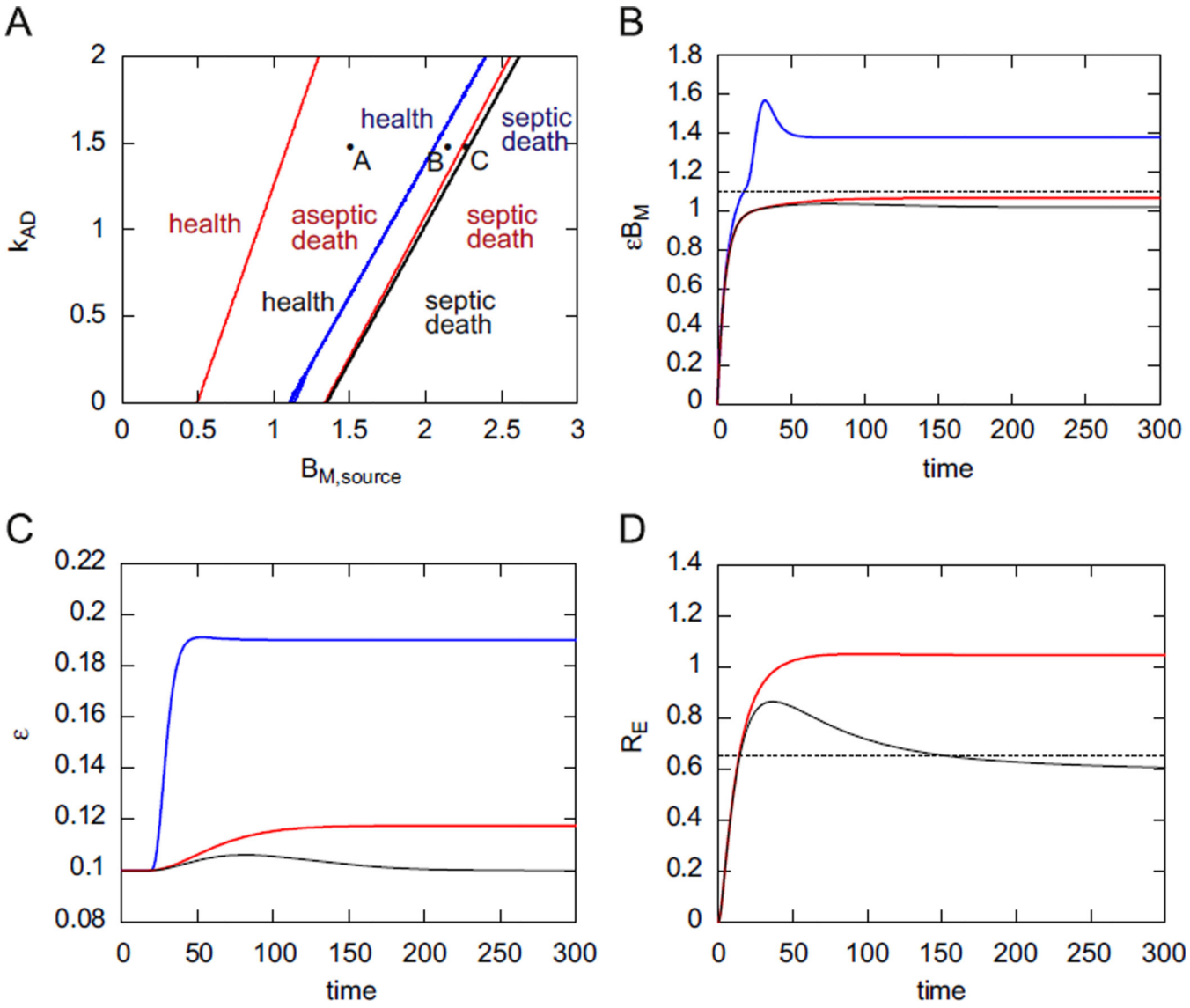

Fig. 8.

Comparison of steady states for Cases 1, 2, and 3. A. Summary of health and disease steady states in k_{AD}–$B_{M,source}$ parameter space (as in Fig. 7B) for Case 1 (blue), Case 2 (red), and Case 3 (black) when a_1 = 0.1/h. The addition of TLR9 to the system (Case 3) restores health to regions that were septic and aseptic in Cases 1 and 2. In particular, the entire region of parameters yielding aseptic death with TLR4 but without TLR9 becomes healthy when TLR9 is included. Three points are labeled to contrast predictions among the three cases: point A ($B_{M,source}$ = 1.5 × 10^6 cells/g/h, k_{AD} = 1.5 × 10^6 cells/g/h), point B ($B_{M,source}$ = 2.2 × 10^6 cells/g/h, k_{AD} = 1.5 × 10^6 cells/g/h), and point C ($B_{M,source}$ = 2.27 × 10^6 cells/g/h, k_{AD} = 1.5 × 10^6 cells/g/h). B. εB_M versus time t for point B. Three cases are colored as in panel A. Dotted line is the value of the εB_M threshold, T. C. ε versus time t. Colors as above. D. R_E (activated TLR4) versus time t. Dotted line is the value of the R_E threshold, T_{RE}. Colors are as above. (For interpretation of the references to color in this figure caption, the reader is referred to the web version of this paper.)

Author Manuscript Author Manuscript Author Manuscript Author Manuscript

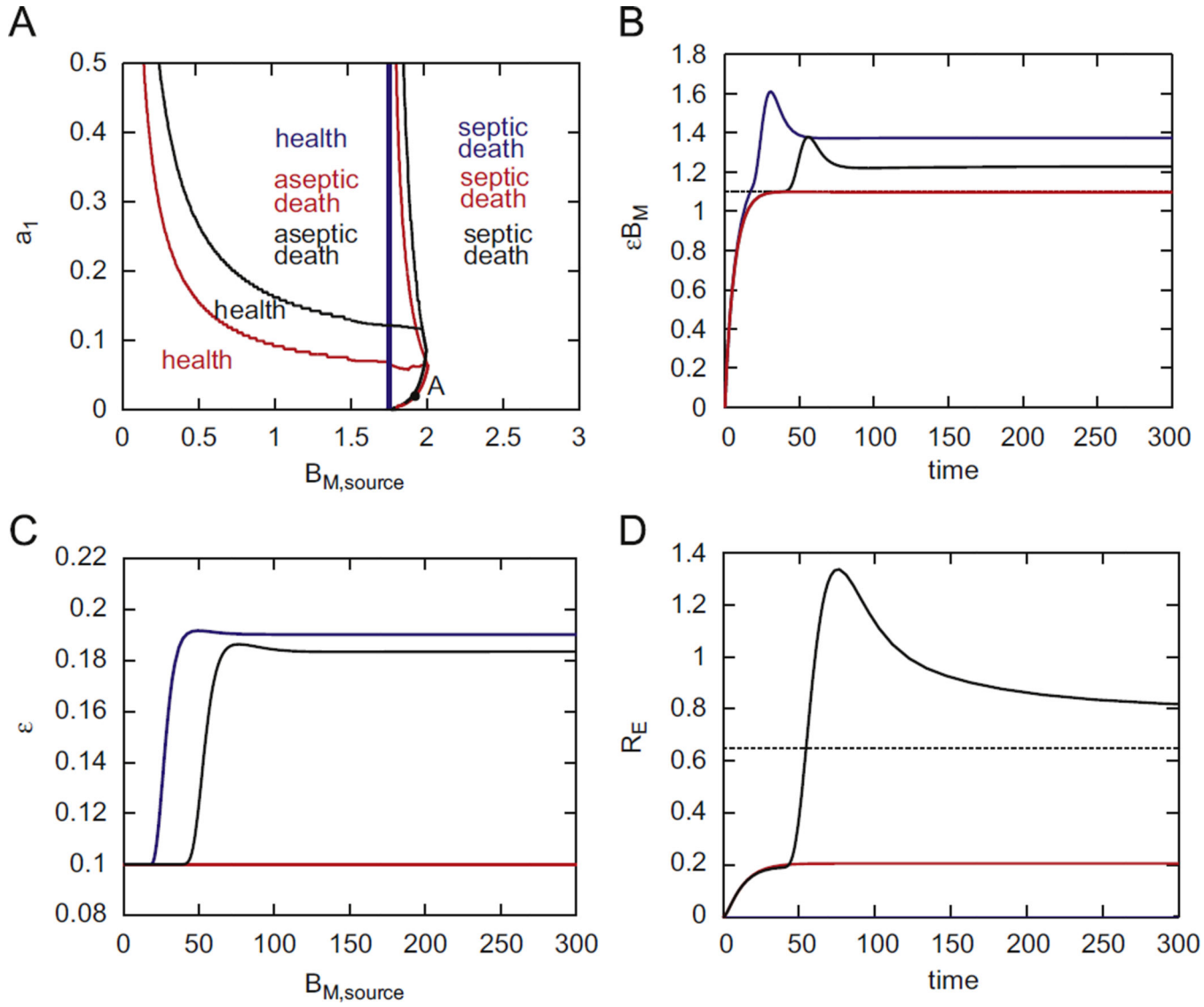

Fig. 9.

Summary of health and disease steady states in a_1−$B_{M,source}$ parameter space for Case 1 (blue), Case 2 (red), and Case 3 (black) when $k_{AD} = 1$. In most of the parameter space, the addition of TLR9 (black curves) expands the region of predicted health. Point A, given by $B_{M,source} = 1.92 \times 10^6$ cells/g/h and $a_1 = 0.02$/h, is an example of a situation in which the presence of TLR4 alone would restore health to an otherwise septic system, yet the additional inclusion of TLR9 hinders the effects of TLR4 and thereby worsens the long-term outcome. B–D. Time courses, as in Fig. 8, for parameter values corresponding to point A. (For interpretation of the references to color in this figure caption, the reader is referred to the web version of this paper.)

Author Manuscript Author Manuscript Author Manuscript Author Manuscript

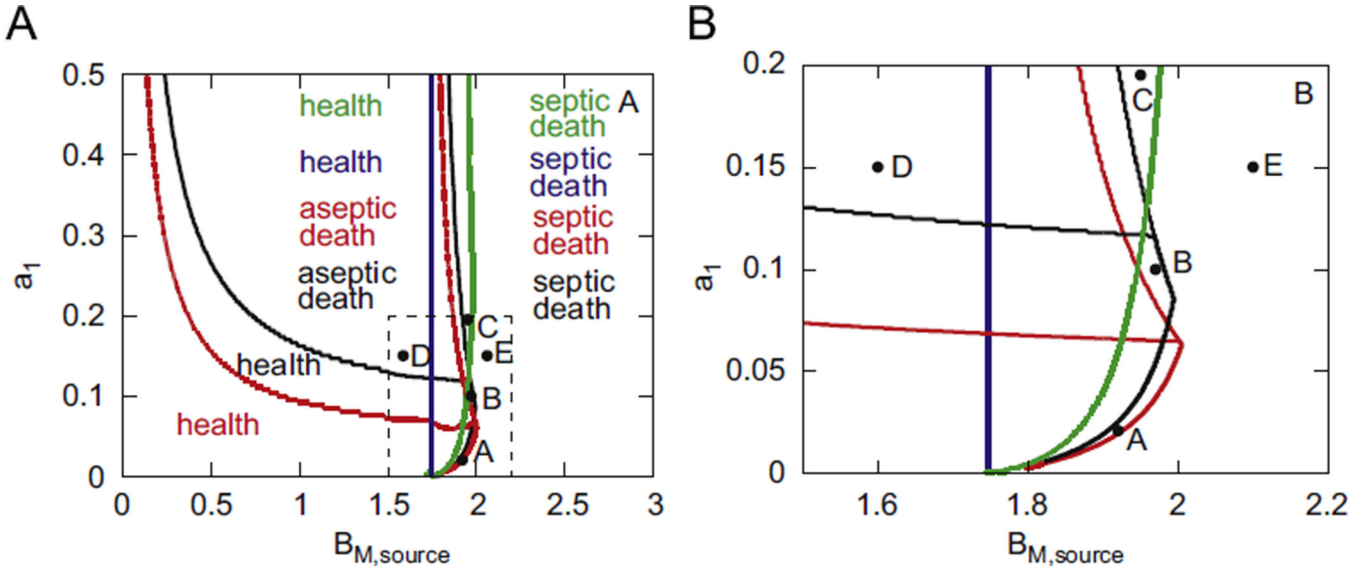

Fig. 10.

Summary of health and disease steady states in a_1–$B_{M,source}$ parameter space, as in Fig. 9A, together with an additional curve (green) showing the effect of increasing parameter k_{IE} to 50 $[I_E]/h$ on the predicted steady states. A. Expanded view, with outcomes labeled in parameter regions where they occur. B. Zoomed view of the region outlined by dashed black lines in A. Labeled points A ($B_{M,source}$ = 1.92 × 10^6 cells/g/h and a_1 = 0.02/h), B ($B_{M,source}$ = 1.97 × 10^6 cells/g/h and a_1 = 0.1/h), C ($B_{M,source}$ = 1.95 × 10^6 cells/g/h and a_1 = 0.195/h), D ($B_{M,source}$ = 1.6 × 10^6 cells/g/h and a_1 = 0.15/h), and E ($B_{M,source}$ = 2.1 × 10^6 cells/g/h and a_1 = 0.15/h) represent several possible effects of TLR4 and TLR9 on observed outcomes (see Table 4 for summary).

Author Manuscript Author Manuscript Author Manuscript Author Manuscript

Table 1

Primers used to determine effects of TLR4 and TLR9 activation.

Model	Primer
mouse TLR4	(F)- GGACTGGGTGAGAAATGAGC
	(R)- GCAATGGCTACACCAGGAAT
mouse TLR9	(F)- GCTGGGACGTCTGGTACTGT
	(R)- ACCACGAAGGCATCATAAGG
rat TLR4	(F)- TGCTCAGACATGGCAGTTTC
	(R)- GCGATACAATTCGACCTGCT
rat TLR9	(F)- CTTCTTTGCTCTGGCGGTAG
	(R)- CGTCAGGTTCATCACAATGG
iNOS	(F)- CTGCTGGTGGTGACAAGCACATTT
	(R)- ATGTCATGAGCAAAGGCGCAGAAC
IL-6	(F)- CCAATTTCCAATGCTCTCCT
	(R)- ACCACAGTGAGGAATGTCCA

Author Manuscript Author Manuscript Author Manuscript Author Manuscript

Table 2

Parameter values for NEC model.

Parameter	Value	Unit	Description
$B_{M,source}$	0–3	10^6 cells/g/h	Rate at which bacteria enter mucus layer
k_{AD}	0–2	10^6 cells/g/h	Maximal rate of bacterial elimination by dendritic cells (DCs)
k_3	6	10^6 cells/g	Half saturation of DC bacterial elimination
k_{AT}	0.03	1/h	Maximal rate of bacterial elimination by TLR4
α_{EM}	0.18	$[R_E]$	Half saturation of TLR4 killing
ε_0	0.1	1/h	Baseline rate of bacterial translocation Han et al. (2004)
ε_{max}	0.21	1/h	Maximum rate of bacterial translocation Han et al. (2004)
τ	24	h	Time scale for epithelial repair
f	0.5	$1/[P]$	Strength of effect of inflammation on bacterial translocation (ε)
a_1	0–0.5	1/h	Maximal rate of activation of TLR4 by bacteria in mucus layer
γ_1	5	10^6 cells/g	Half saturation of TLR4 activation by mucosal bacteria (B_M)
k_1	0.5	$[R_E]/[P]$/h	Maximal rate of TLR4 activation by pro-inflammatory cytokines (P)
α_{RE}	2	$1/[I_E]$	Strength of inhibitory effect of TLR9 on TLR4 activation by B_M and P
μ_{RE}	0.1	1/h	Decay rate of TLR4
k_{IE}	0–50	$[I_E]/h$	Maximal rate of activation of TLR9 by activated TLR4
γ_{IE}	10	$[R_E]$	Half saturation of TLR9 activation
α_{11}	0.1	$[I_E]/h$	Rate of activation of TLR9 directly by bacteria
μ_{IE}	1	1/h	Decay rate of TLR9
T	1.1	10^6 cells/g/h	Epithelial barrier threshold
k_5	25	$1/h/[P]$	Rate of bacterial elimination by cytokines
k_{PM}	0.8	$[P]$/h	Max rate of production of P in response to blood/tissue bacteria (B)
γ_{12}	1.2	10^6 cells/g	Half saturation of P production
k_{PE}	0.002	1/h	Maximal rate of production of P by TLR4
T_{RE}	0.65	$[R_E]$	Threshold for TLR4 to begin pro-inflammatory cytokine production
γ_{PE}	1	$1/[I_E]$	Strength of TLR9 inhibition of P production
μ_4	0.05	1/h	Decay rate of P

Author Manuscript Author Manuscript Author Manuscript Author Manuscript

Table 3

Summary of steady state behavior at points A, B, and C in Fig. 8. Case 1: no TLR4 and no TLR9. Case 2: with TLR4 and no TLR9. Case 3: with TLR4 and with TLR9.

Point	Case	εB_M	ε	R_E	B	Summary
	1	$< T$	ε_0	–	0	Health
A (1.5, 1.5)	2	$< T$	$> \varepsilon_0$	$> T_{RE}$	0	Aseptic
	3	$< T$	ε_0	$< T_{RE}$	0	Health
	1	$> T$	$> \varepsilon_0$	–	> 0	Septic
B (2.2, 1.5)	2	$< T$	$> \varepsilon_0$	$> T_{RE}$	0	Aseptic
	3	$< T$	ε_0	$< T_{RE}$	0	Health
	1	$> T$	ε_0	–	> 0	Septic
C (2.27, 1.5)	2	$> T$	$> \varepsilon_0$	$> T_{RE}$	> 0	Septic
	3	$< T$	ε_0	$< T_{RE}$	0	Health

Author Manuscript Author Manuscript Author Manuscript Author Manuscript

Table 4

Summary of steady state behavior at points A, B, C, D, and E in Fig. 10 for the following four scenarios: Case 1 – no TLR4 and no TLR9, Case 2 – with TLR4 and no TLR9, Case 3 - with TLR4 and with TLR9, and Treatment – increasing value of parameter k_{IE}.

Case	Point A	Point B	Point C	Point D	Point E
1	Septic	Septic	Septic	Health	Septic
2	Health	Septic	Septic	Aseptic	Septic
3	Septic	Health	Septic	Aseptic	Septic
Treatment	Septic	Septic	Health	Health	Septic

Author Manuscript

Author Manuscript

Author Manuscript

Author Manuscript

Table 5

Summary of scenarios in which potential treatment strategies for NEC are not successful. Three proposed treatments for NEC are listed: reduce bacteria in the mucus layer (decrease $B_{M,source}$), administer probiotics (increase k_{IE}), and block TLR4 (decrease a_1). In most cases, the model predicts that all three treatments will restore health in previously aseptic or septic cases. However, this provides a summary of scenarios in which proposed treatment is not predicted to restore a healthy steady state in each of the mathematical case studies.

Case	Decreasing $B_{M,source}$	Increasing k_{IE}	Decreasing a_1
1	$B_M(0)$ high (initially above T)	NA	NA
2	a_1 too high (Fig. 7D)	NA	$B_{M,source}$ too high; decreased a_1 too much (Fig. 9A)
3	a_1 too high (Fig. 9A)	Specific combination of $B_{M,source}$ and a_1 (Fig. 10A)	$B_{M,source}$ too high; decreased a_1 too much (Fig. 9A)